Проблемы и вызовы физики космических лучей ультравысоких энергий

Объединенный семинар ОФВЭ и ОТФ ПИЯФ,
18 мая 2023 г.

Г.И. Рубцов
Институт ядерных исследований РАН
коллаборация Telescope Array

фото Олега Калашева

План доклада

- Установки, регистрирующие космические лучи ультравысоких энергий
- Энергетический спектр
- Химический состав и адронные взаимодействия
- Проблема мюонного избытка
- Поиск источников
- Междисциплинарные результаты

Установки, регистрирующие космические лучи $E>10^{18}$ эВ

Якутск ШАЛ

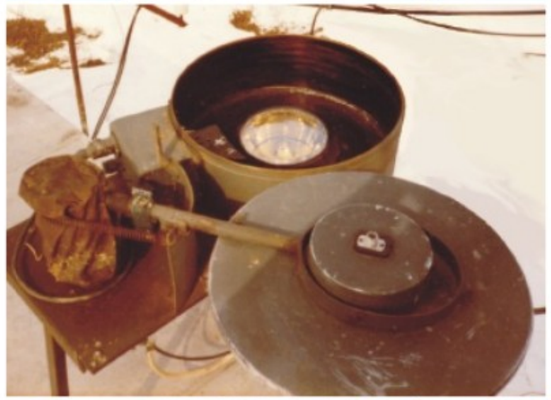

Pierre Auger

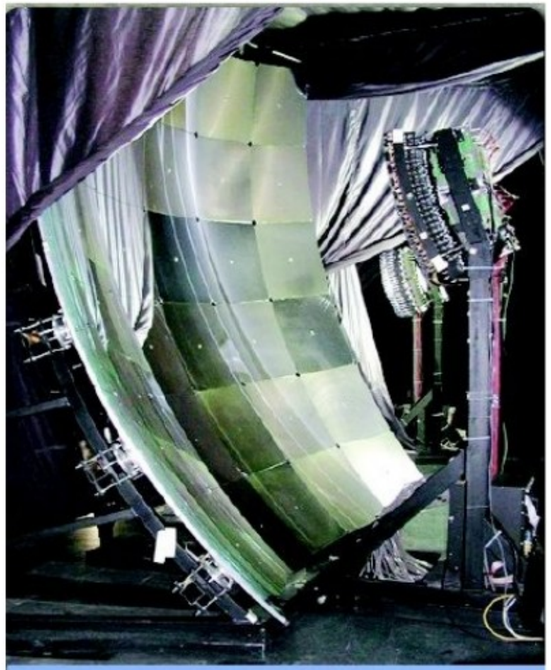

Telescope Array

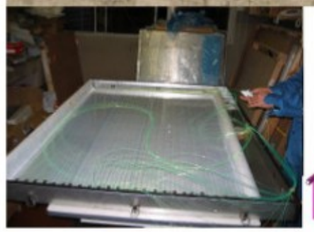

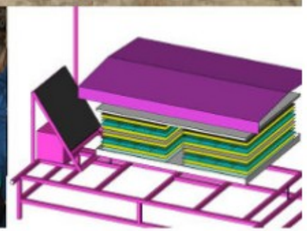

The Pierre Auger Observatory

Pierre Auger Observatory
Province Mendoza, Argentina

Radio antenna array
(153 antennas, 17 km²)

Underground muon
detectors (24+)

Sub-array of 750 m
(63 stations, 23.4 km²)

LIDARs and laser facilities

High elevation telescopes (3)

4 fluorescence detectors
(24 telescopes up to 30°)

Central
Campus

1665 surface detectors:
water-Cherenkov tanks
(grid of 1.5 km, 3000 km²)

**More than 400 members,
98 institutes, 17 countries**

**Southern hemisphere: Malargue,
Province Mendoza, Argentina**

**Water-Cherenkov
detectors and**

**Fluorescence
telescopes**

Telescope Array: крупнейшая в Северном полушарии обсерватория, регистрирующая КЛ

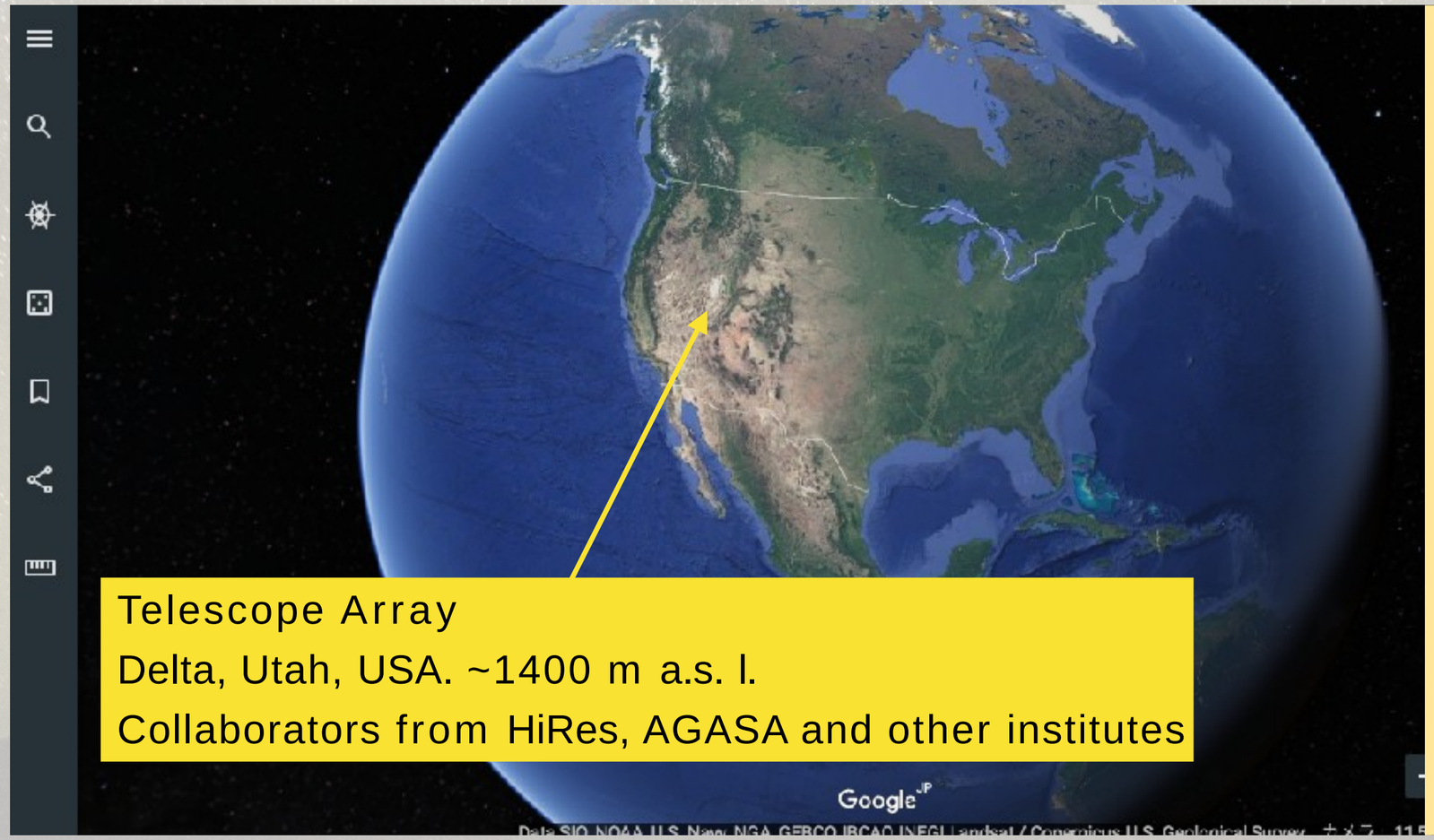

Science goals:

- Origin and properties of the ultra-high energy cosmic rays:
  - spectrum, composition, anisotropy
- Physics of HE hadronic interactions
- Multi-messenger and interdisciplinary studies
  - photons, neutrino, dark matter
  - thunderstorms, TGFs
  - meteoroids
- Development of the next generation experiments

Telescope Array Collaboration

R.U. Abbasi[1,2], M. Abe[3], T. Abu-Zayyad[1,2], M. Allen[2], Y. Arai[4], R. Arimura[4], E. Barcikowski[2], J.W. Belz[2], D.R. Bergman[2], S.A. Blake[2], I. Buckland[2], R. Cady[2], B.G. Cheon[5], J. Chiba[6], M. Chikawa[7], T. Fujii[8], K. Fujisue[7], K. Fujita[4], R. Fujiwara[4], M. Fukushima[7], R. Fukushima[4], G. Furlich[2], R. Gonzalez[2], W. Hanlon[2], M. Hayashi[9], N. Hayashida[10], K. Hibino[10], R. Higuchi[7], K. Honda[11], D. Ikeda[10], T. Inadomi[12], N. Inoue[3], T. Ishii[11], H. Ito[13], D. Ivanov[2], H. Iwakura[12], A. Iwasaki[4], H.M. Jeong[14], S. Jeong[14], C.C.H. Jui[2], K. Kadota[15], F. Kakimoto[10], O. Kalashev[16], K. Kasahara[17], S. Kasami[18], H. Kawai[19], S. Kawakami[4], S. Kawana[3], K. Kawata[7], I. Kharuk[16], E. Kido[13], H.B. Kim[5], J.H. Kim[2], J.H. Kim[2], M.H. Kim[14], S.W. Kim[14], Y. Kimura[4], S. Kishigami[4], Y. Kubota[12], S. Kurisu[12], V. Kuzmin[16], M. Kuznetsov[16,20], Y.J. Kwon[21], K.H. Lee[14], B. Lubsandorzhiev[16], J.P. Lundquist[2,22], K. Machida[11], H. Matsumiya[4], T. Matsuyama[4], J.N. Matthews[2], R. Mayta[4], M. Minamino[4], K. Mukai[11], I. Myers[2], S. Nagataki[13], K. Nakai[4], R. Nakamura[12], T. Nakamura[23], T. Nakamura[12], Y. Nakamura[12], A. Nakazawa[12], T. Nonaka[7], H. Oda[4], S. Ogio[4,24], M. Ohnishi[7], H. Ohoka[7], Y. Oku[18], T. Okuda[25], Y. Omura[4], M. Ono[13], R. Onogi[4], A. Oshima[4], S. Ozawa[26], I.H. Park[14], M. Potts[2], M.S. Pshirkov[16,27], J. Remington[2], D.C. Rodriguez[2], G.I. Rubtsov[16], D. Ryu[28], H. Sagawa[7], R. Sahara[4], Y. Saito[12], N. Sakaki[7], T. Sako[7], N. Sakurai[4], K. Sano[12], K. Sato[4], T. Seki[12], K. Sekino[7], P.D. Shah[2], Y. Shibasaki[12], F. Shibata[11], N. Shibata[18], T. Shibata[7], H. Shimodaira[7], B.K. Shin[28], H.S. Shin[7], D. Shinto[18], J.D. Smith[2], P. Sokolsky[2], N. Sone[12], B.T. Stokes[2], T.A. Stroman[2], T. Suzawa[3], Y. Takagi[4], Y. Takahashi[4], M. Takamura[6], M. Takeda[7], R. Takeishi[7], A. Taketa[29], M. Takita[7], Y. Tameda[18], H. Tanaka[4], K. Tanaka[30], M. Tanaka[31], Y. Tanoue[4], S.B. Thomas[2], G.B. Thomson[2], P. Tinyakov[16,20], I. Tkachev[16], H. Tokuno[32], T. Tomida[12], S. Troitsky[16], R. Tsuda[4], Y. Tsunesada[4,24], Y. Uchihori[33], S. Udo[10], T. Uehama[12], F. Urban[34], T. Wong[2], K. Yada[7], M. Yamamoto[12], K. Yamazaki[10], J. Yang[35], K. Yashiro[6], F. Yoshida[18], Y. Yoshioka[12], Y. Zhezher[7,16], and Z. Zundel[2]

[1] Loyola University Chicago [2] University of Utah [3] Saitama University [4] Osaka City University [5] Hanyang University [6] Tokyo University of Science [7] University of Tokyo (ICRR) [8] Kyoto University [9] Shinshu University [10] Kanagawa University [11] University of Yamanashi [12] Shinshu University (Inst. of Engineering) [13] RIKEN [14] Sungkyunkwan University [15] Tokyo City University [16] Institute for Nuclear Research of the Russian Academy of Sciences [17] Shibaura Institute of Technology [18] Osaka Electro-Communication University [19] Chiba University [20] Université Libre de Bruxelles [21] Yonsei University [22] University of Nova Gorica [23] Kochi University [24] Osaka City University (Nambu Yoichiro Institute) [25] Ritsumeikan University [26] National Inst. for Information and Communications Technology, Tokyo [27] Lomonosov Moscow State University [28] Ulsan National Institute of Science and Technology [29] University of Tokyo (Earthquake Inst.) [30] Hiroshima City University [31] KEK [32] Tokyo Institute of Technology [33] National Instit. for Quantum and Radiological Science and Technology [34] CEICO, Institute of Physics, Czech Academy of Sciences [35] Ewha Womans University

160 members , 35 institutes, 7 countries


USA

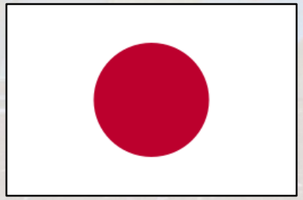
Japan


Korea


Russia


Belgium


Czech Republic

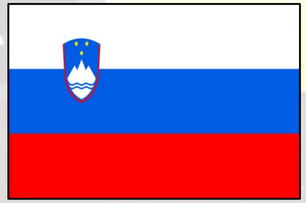
Slovenia

Map of the TA site

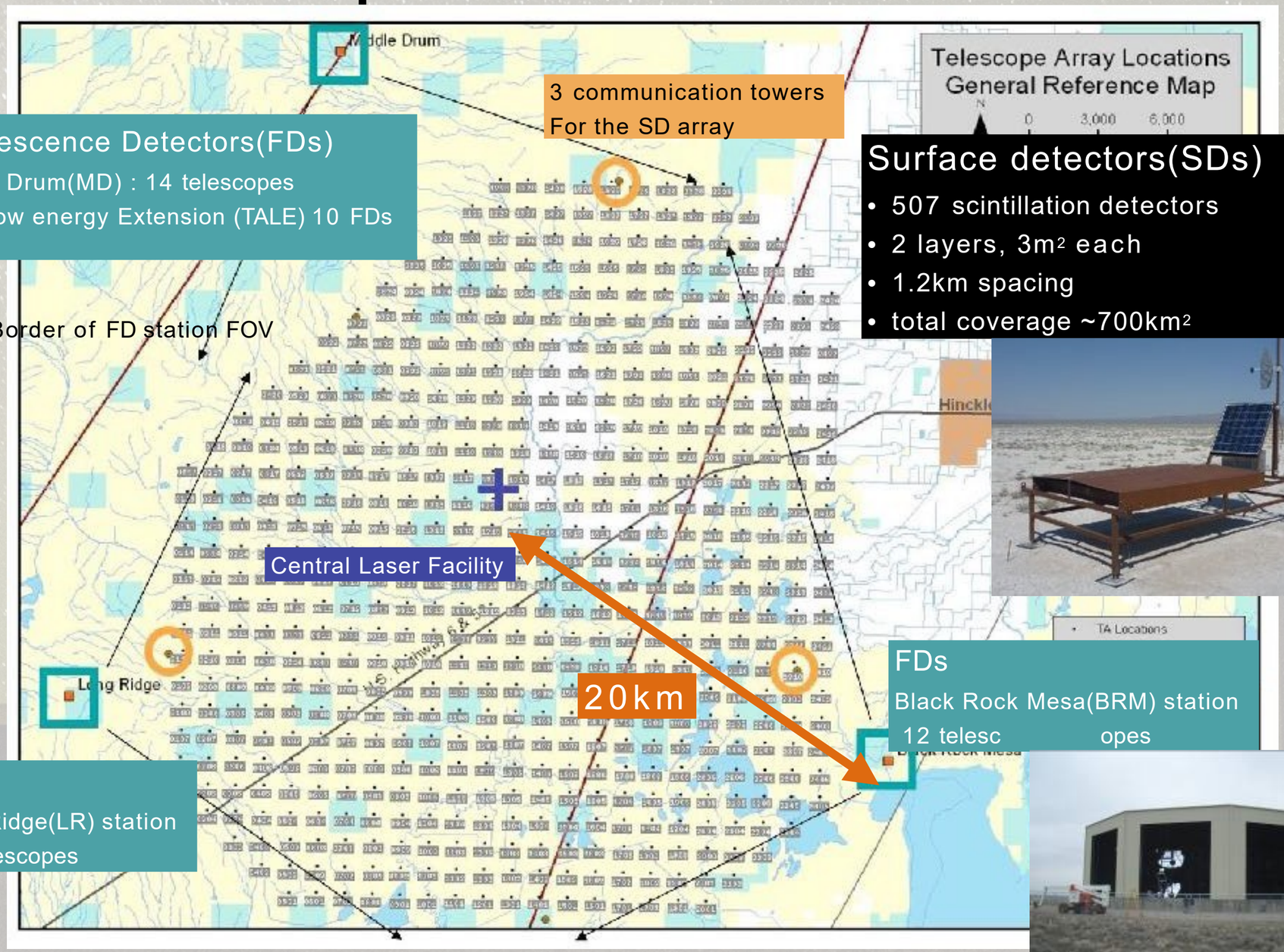

Fluorescence Detectors(FDs)
Middle Drum(MD) : 14 telescopes
+ TA Low energy Extension (TALE) 10 FDs

3 communication towers
For the SD array

Surface detectors(SDs)
- 507 scintillation detectors
- 2 layers, 3m² each
- 1.2km spacing
- total coverage ~700km²

Border of FD station FOV

Central Laser Facility

FDs
Black Rock Mesa(BRM) station
12 telesc opes

FDs
Long Ridge(LR) station
12 telescopes

TALE

Located in TA MD site
10 FDs in the TALE station
Elevation: 30◦-57◦ (higher elevation than MD) Azimuthal: 114◦

104 SD infill array identical to main TA SD
Variable spacing up to 400m

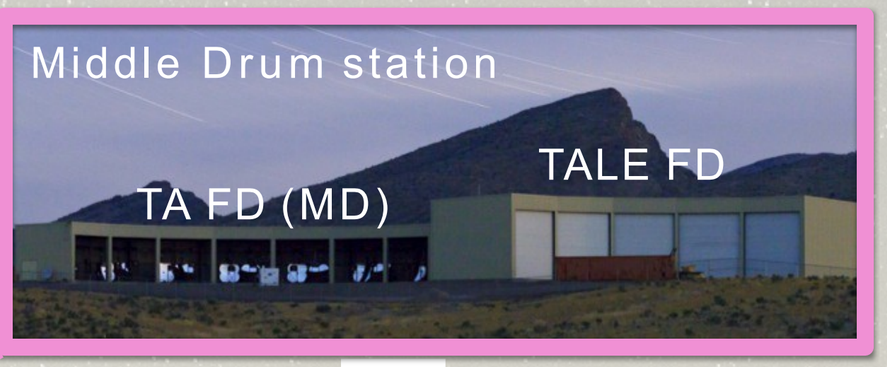

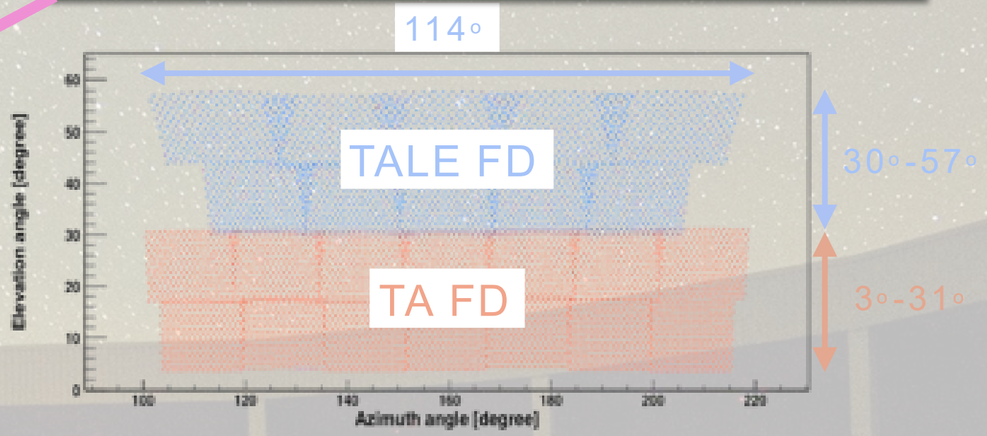

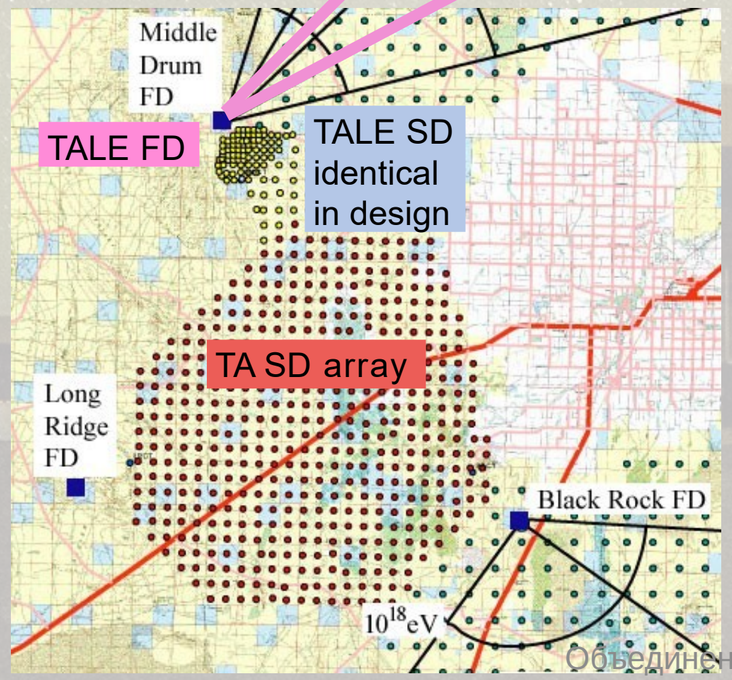

TALE FD Installed in Nov. 2012
Operation since Sep. 2013

TALE SD completed Mar. 2018
Hybrid trigger: Sep. 2018

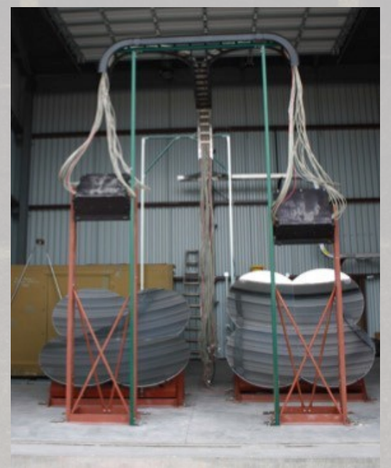

TA×4

TA×4 northern FD station

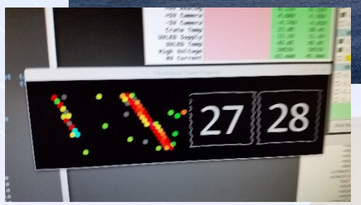

routine observation
since Jun. 2019

TA×4 southern FD station

routine observation
since Aug. 2020

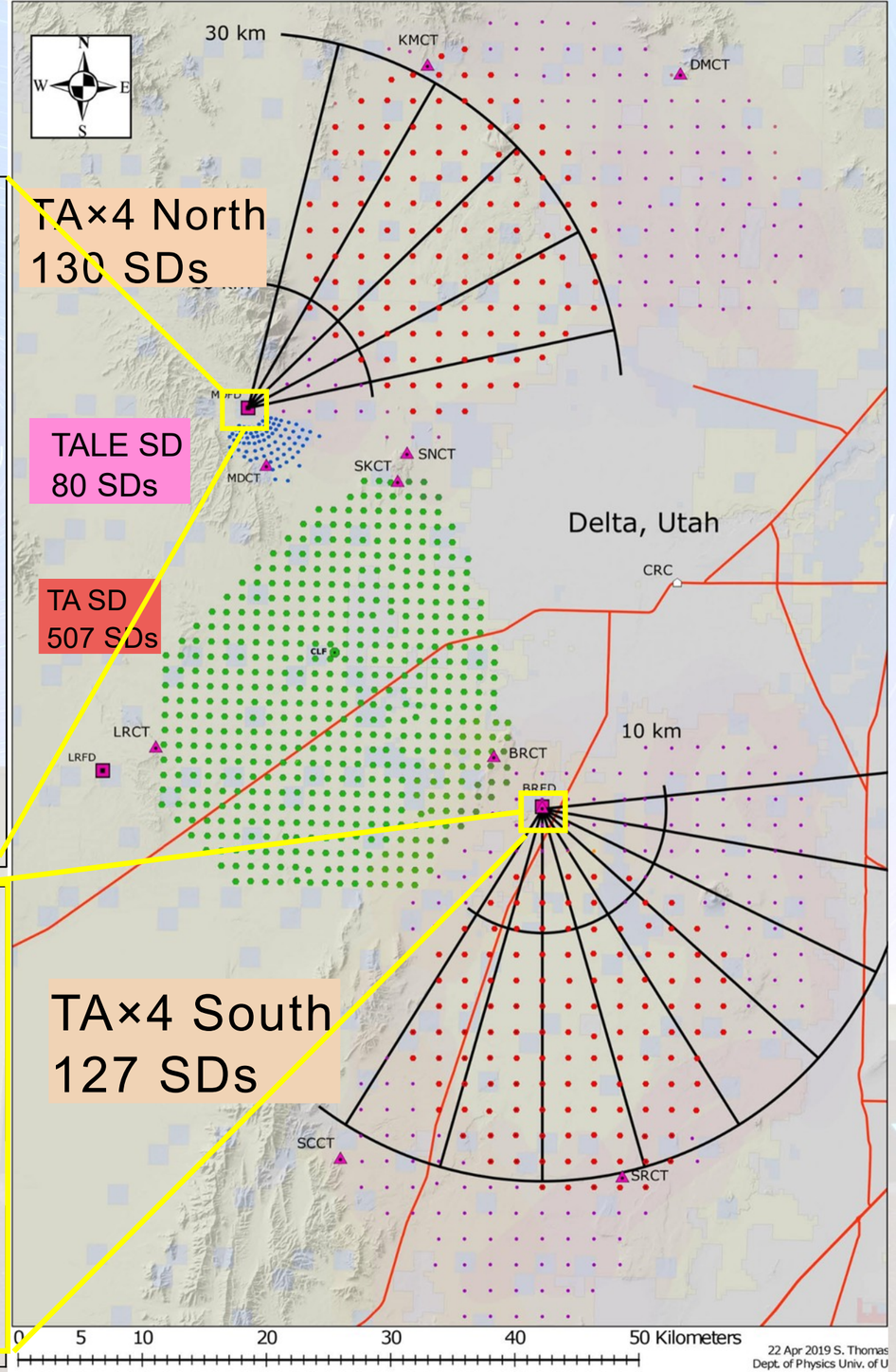

- Goal: fourfold increase in size of TA SD array (up to 3000 km^2).
- Triple statistics for E>20 EeV in 5 years.

- Hybrid experiment:
- 2 FD stations, 12 telescopes are installed

- 257 SD scintillators out of 500 are installed and operational since Nov. 2019

SD Event Reconstruction

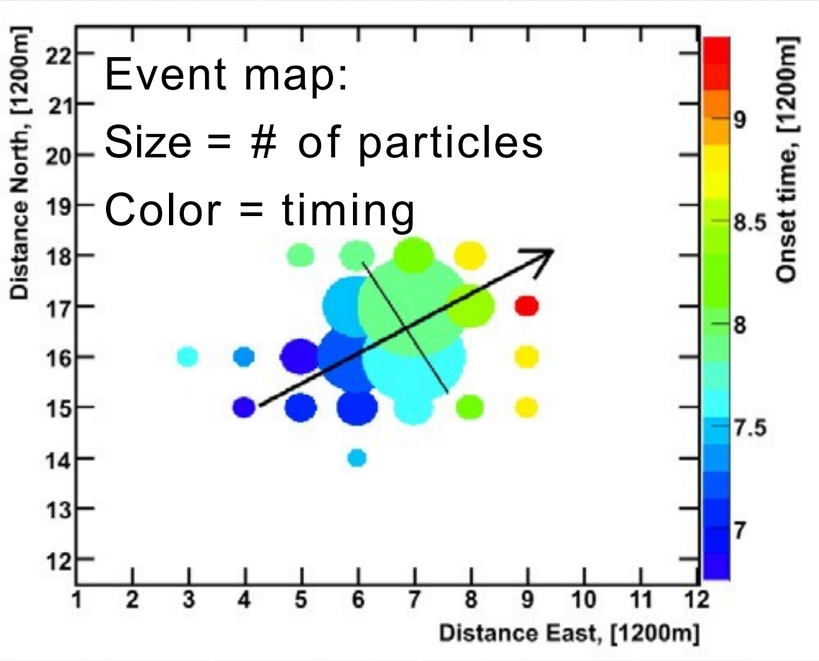

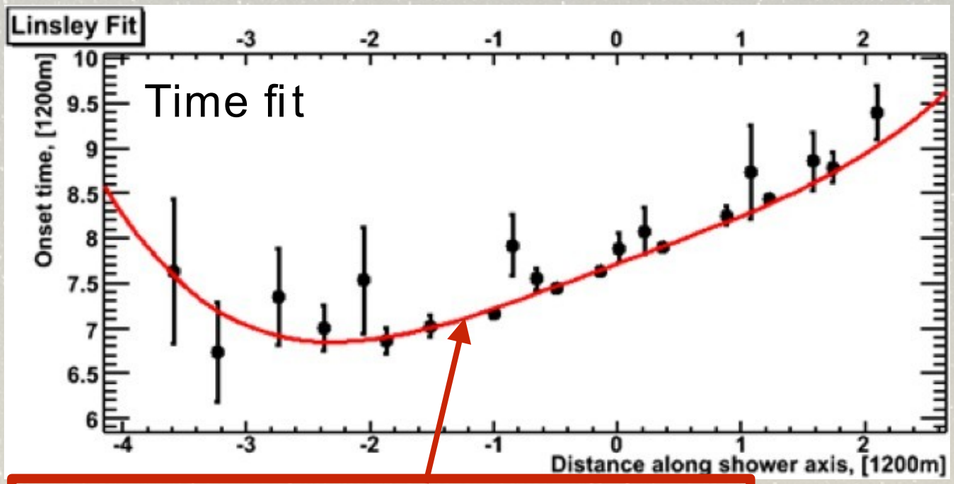

$$\tau = a\left(1-\frac{l}{12\times10^{3}\mathrm{m}}\right)^{1.05}\left(1.0+\frac{s}{30\mathrm{m}}\right)^{1.35}\rho^{-0.5}$$

Modified empirical formula in AGASA

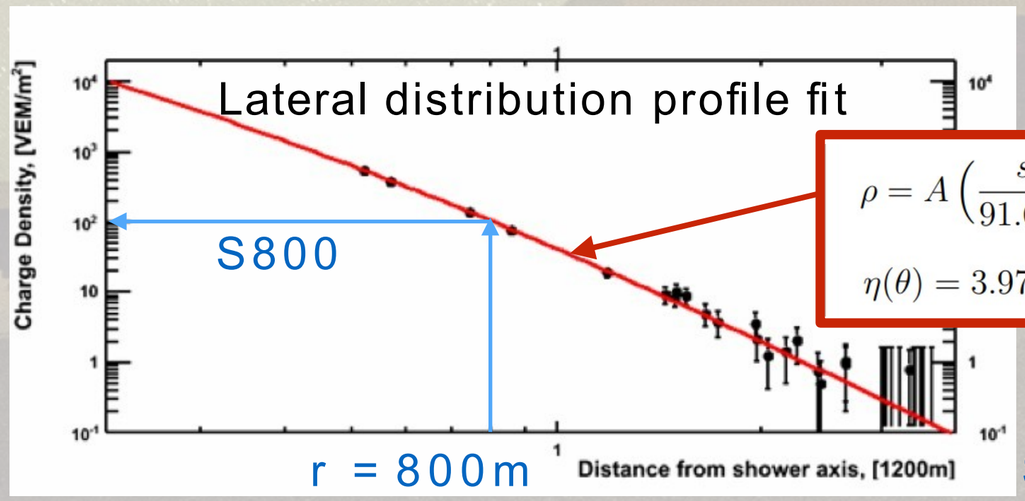

$$\rho = A\left(\frac{s}{91.6\mathrm{m}}\right)^{-1.2}\left(1+\frac{s}{91.6\mathrm{m}}\right)^{-(\eta(\theta)-1.2)}\left(1+\left[\frac{s}{1000\mathrm{m}}\right]^{2}\right)^{-0.6}$$

$$\eta(\theta) = 3.97 - 1.79\,[\sec(\theta)-1]$$

Empirical formula used by AGASA

S800 -> primary energy

Event reconstruction

Stereo

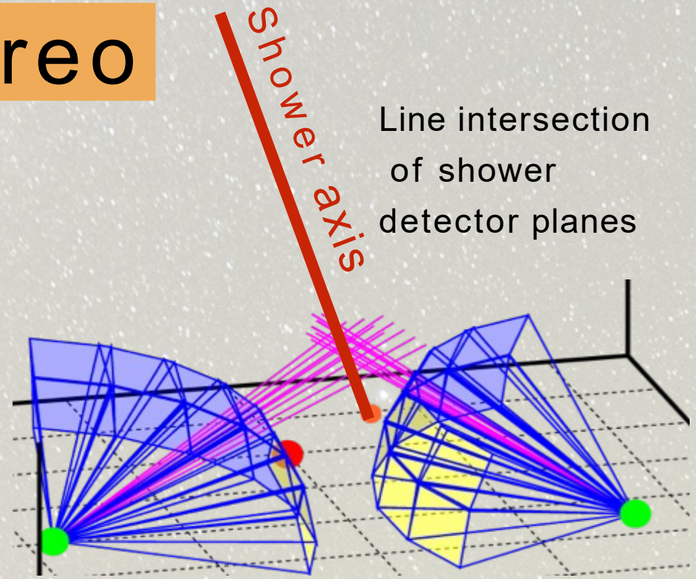

observed images

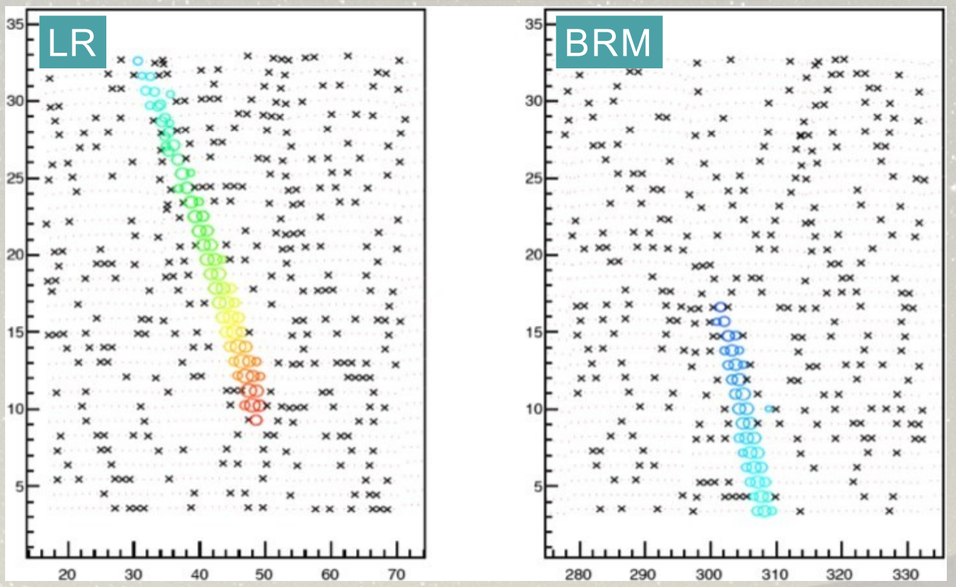

Hybrid

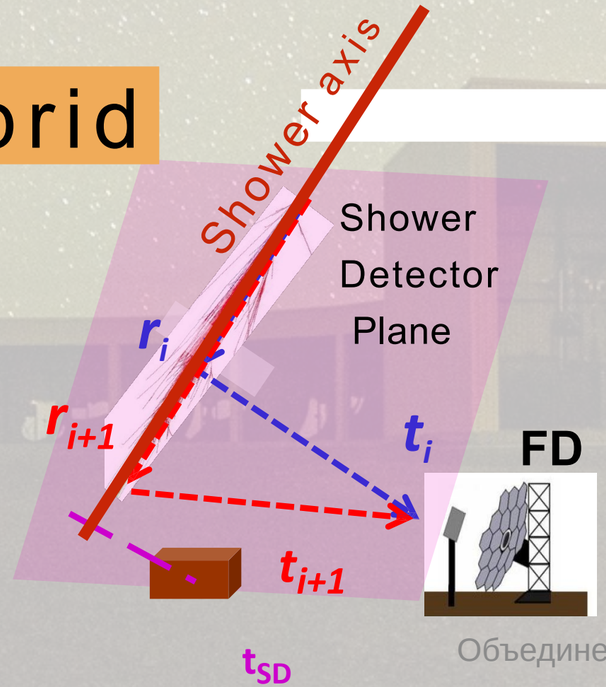

reconstructed shower profiles

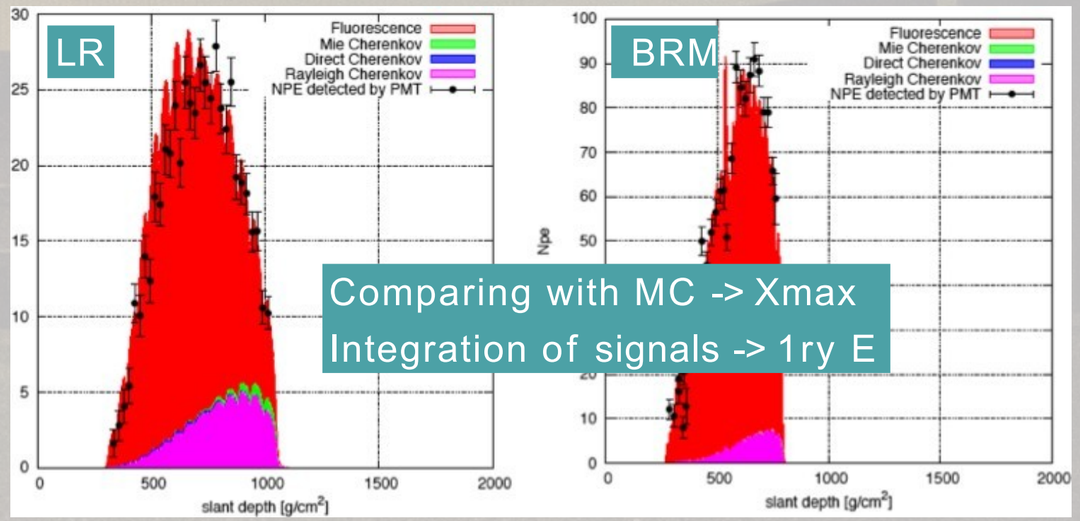

TAx4 Hybrid Event Example

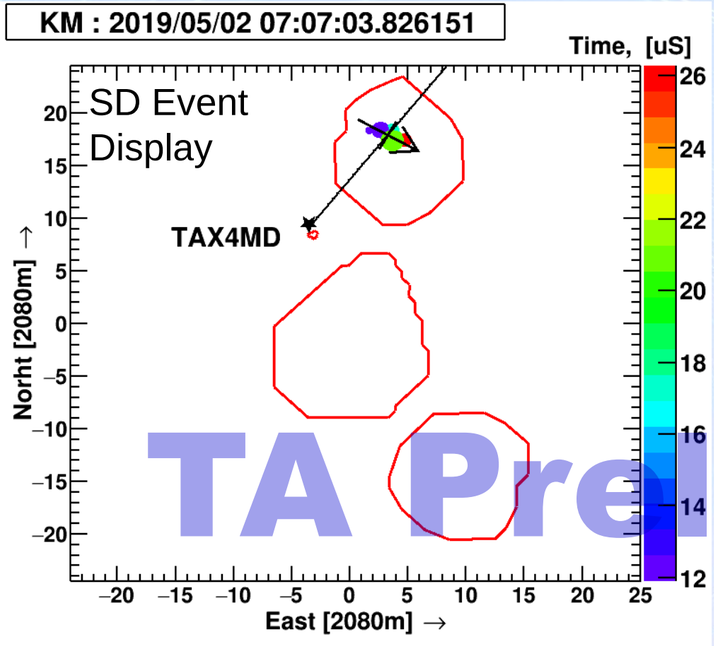

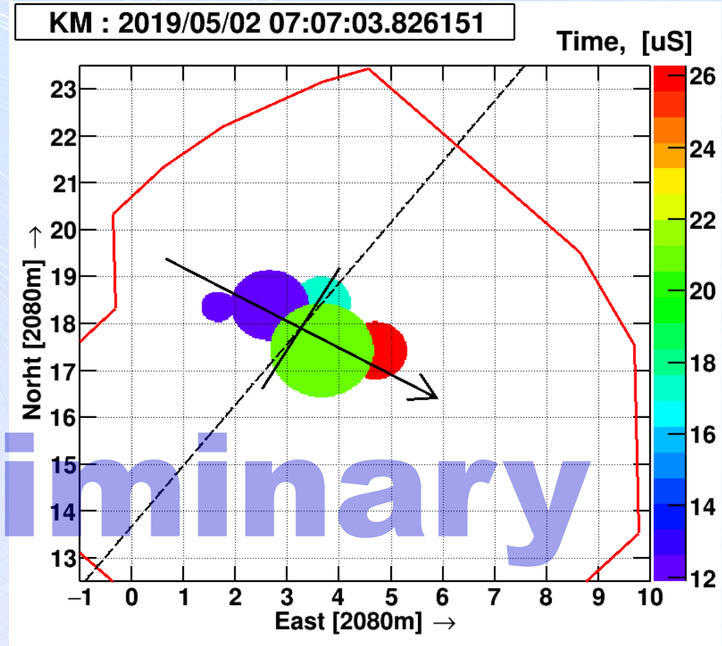

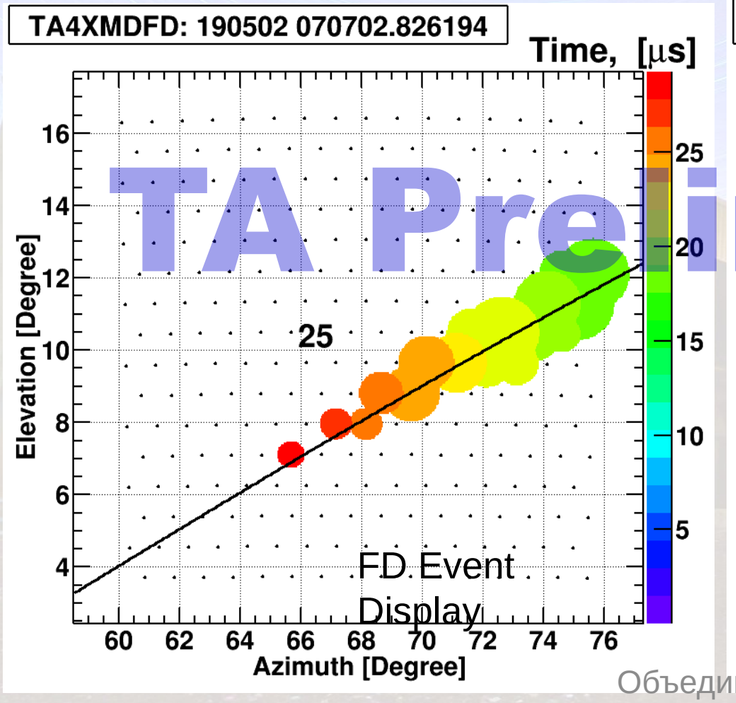

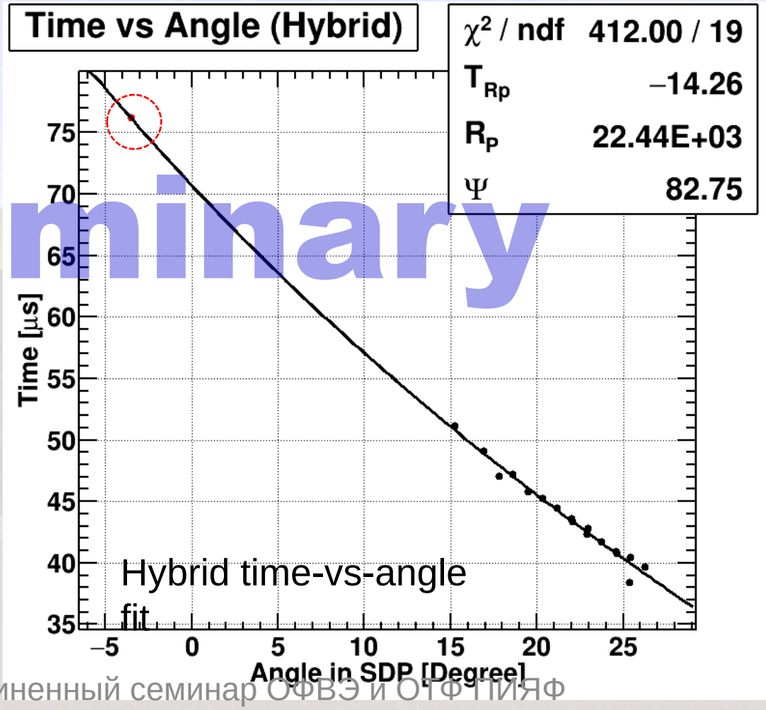

Энергетический спектр

TA SD Energy Spectrum

TA SD 14 years data

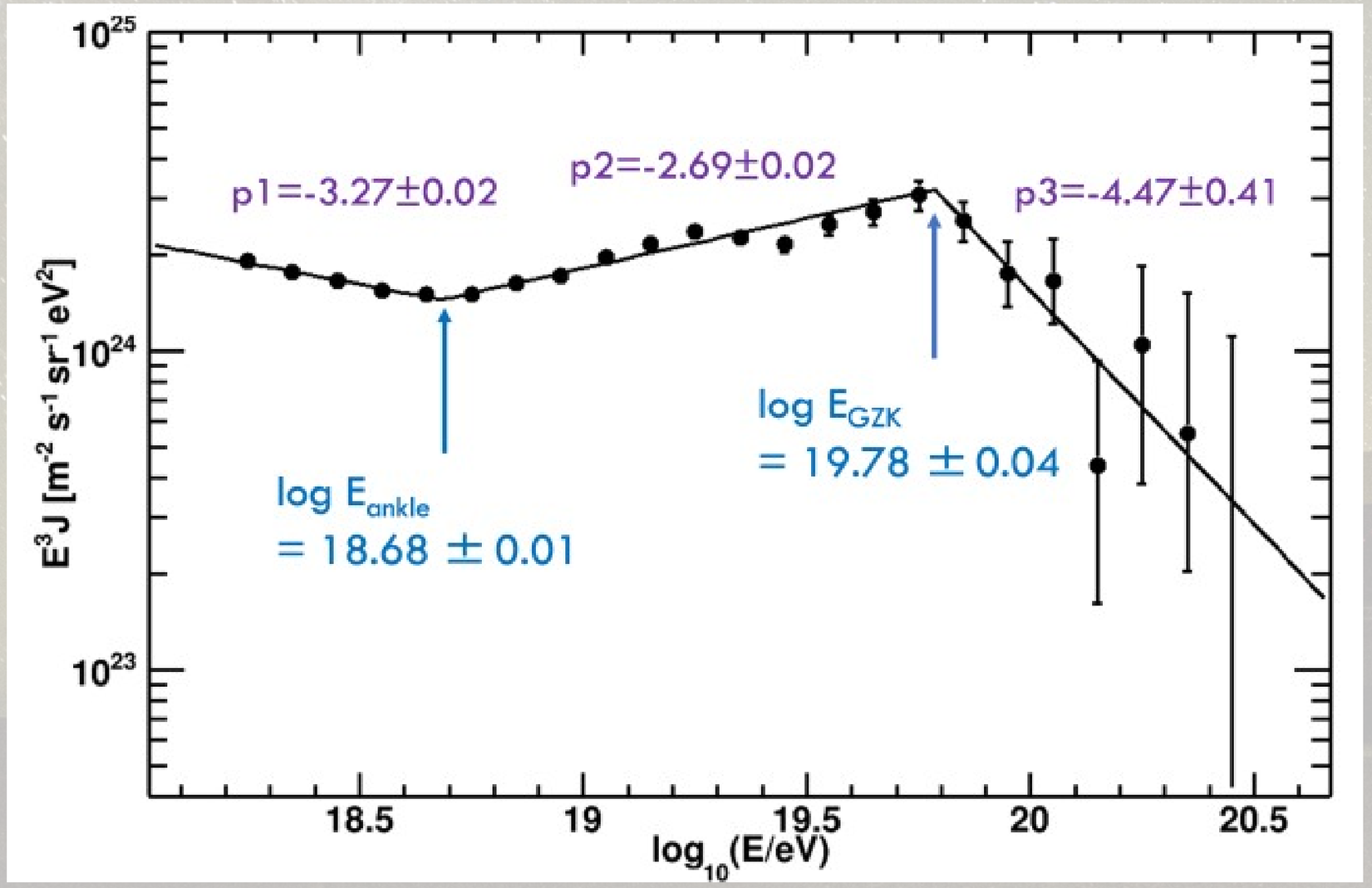

TAx4 SD 2 years (preliminary)

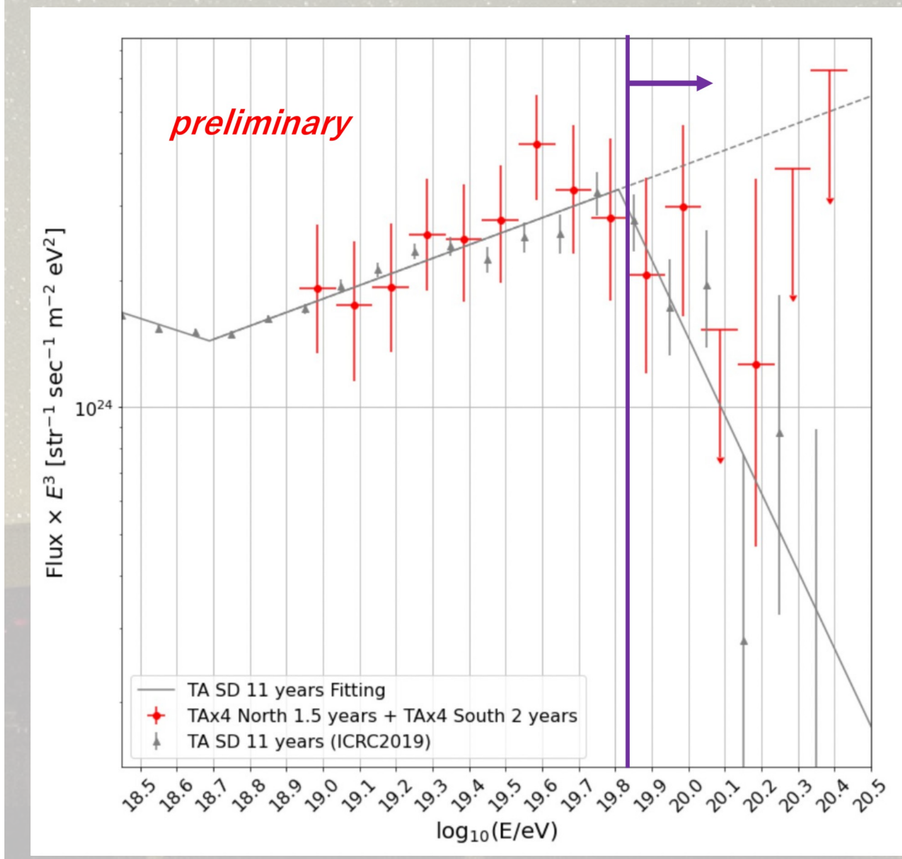

New spectral feature (softening)

TA SD 14 years spectrum

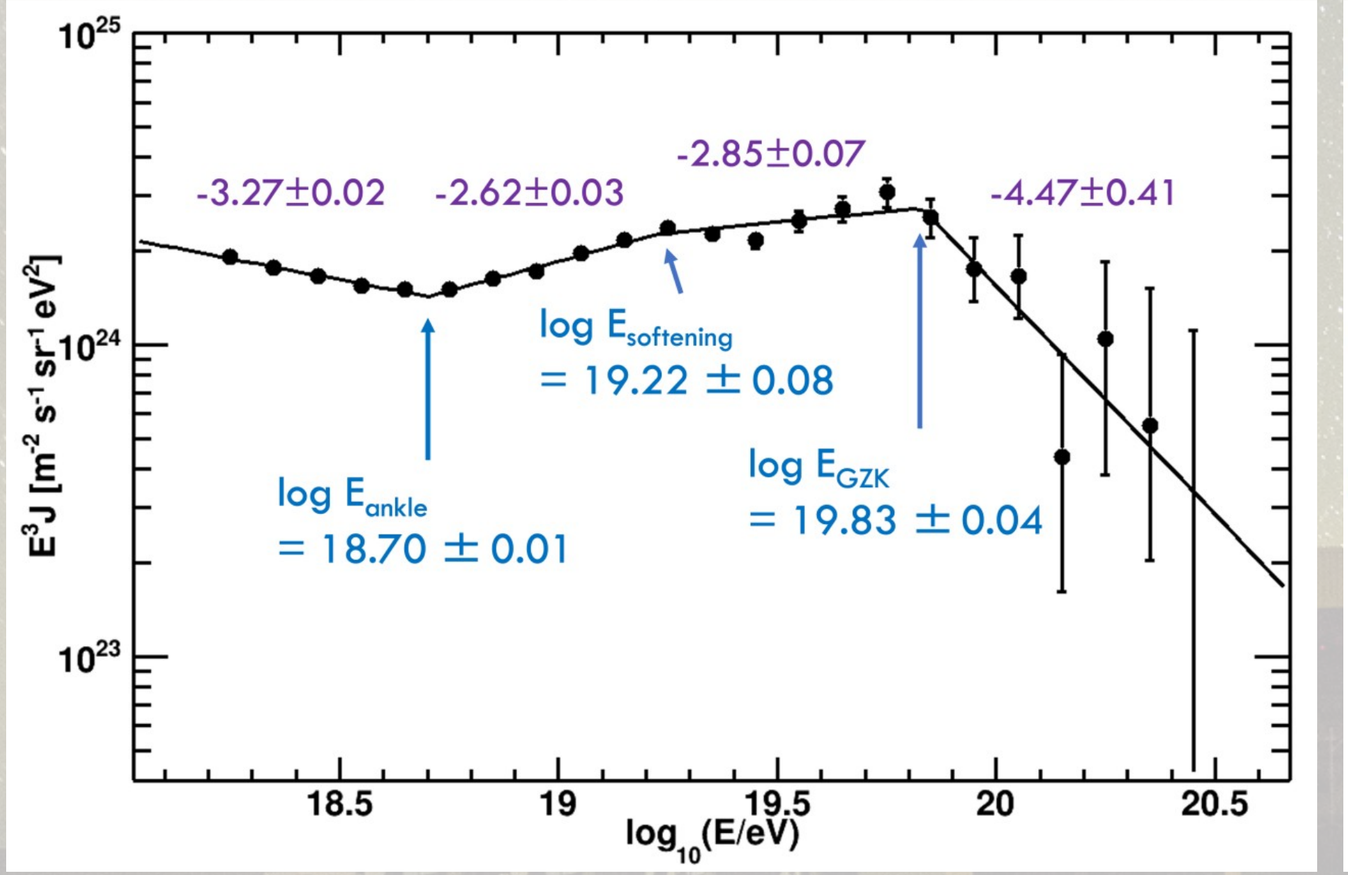

Pierre Auger spectrum

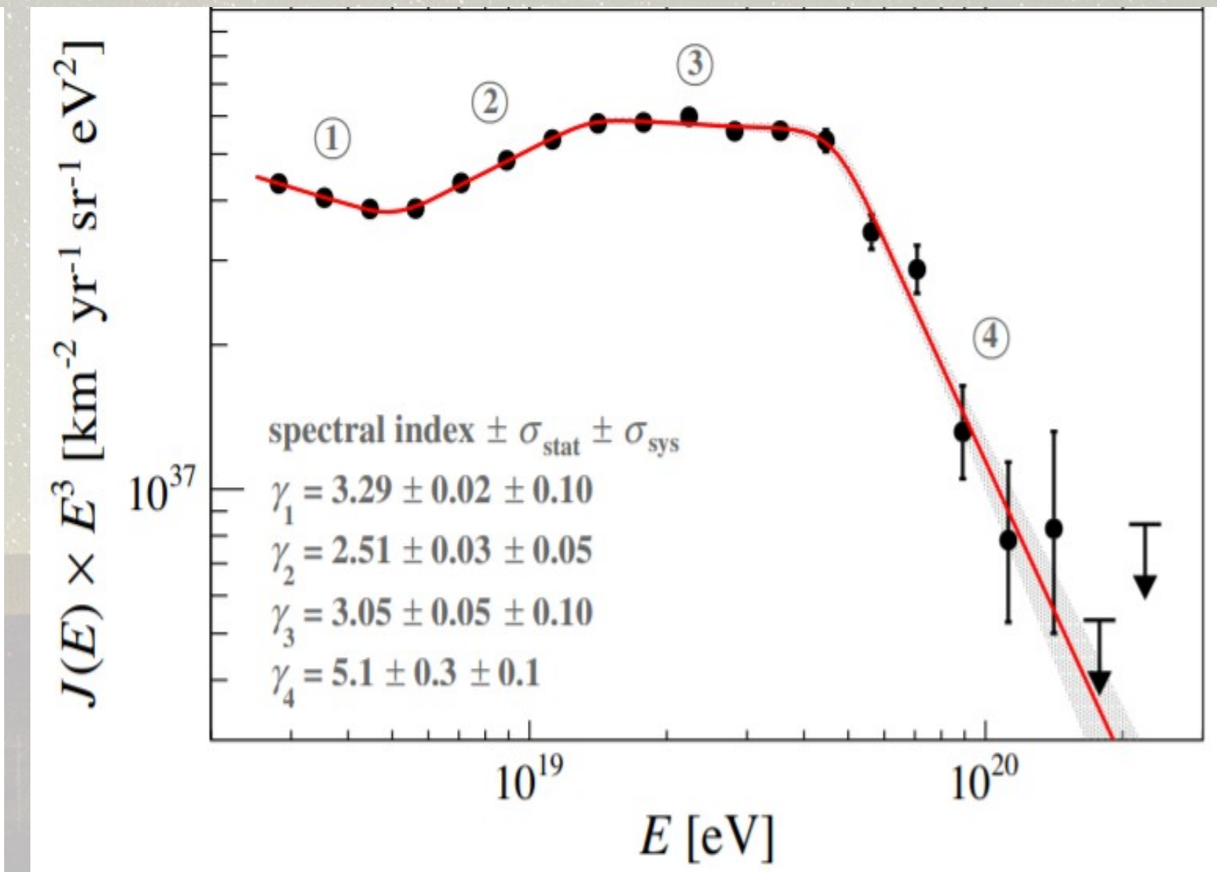

A. Aab *et al.* (The Pierre Auger Collaboration)
Phys. Rev. Lett. **125**, 121106 (2020)

Combined Energy Spectrum

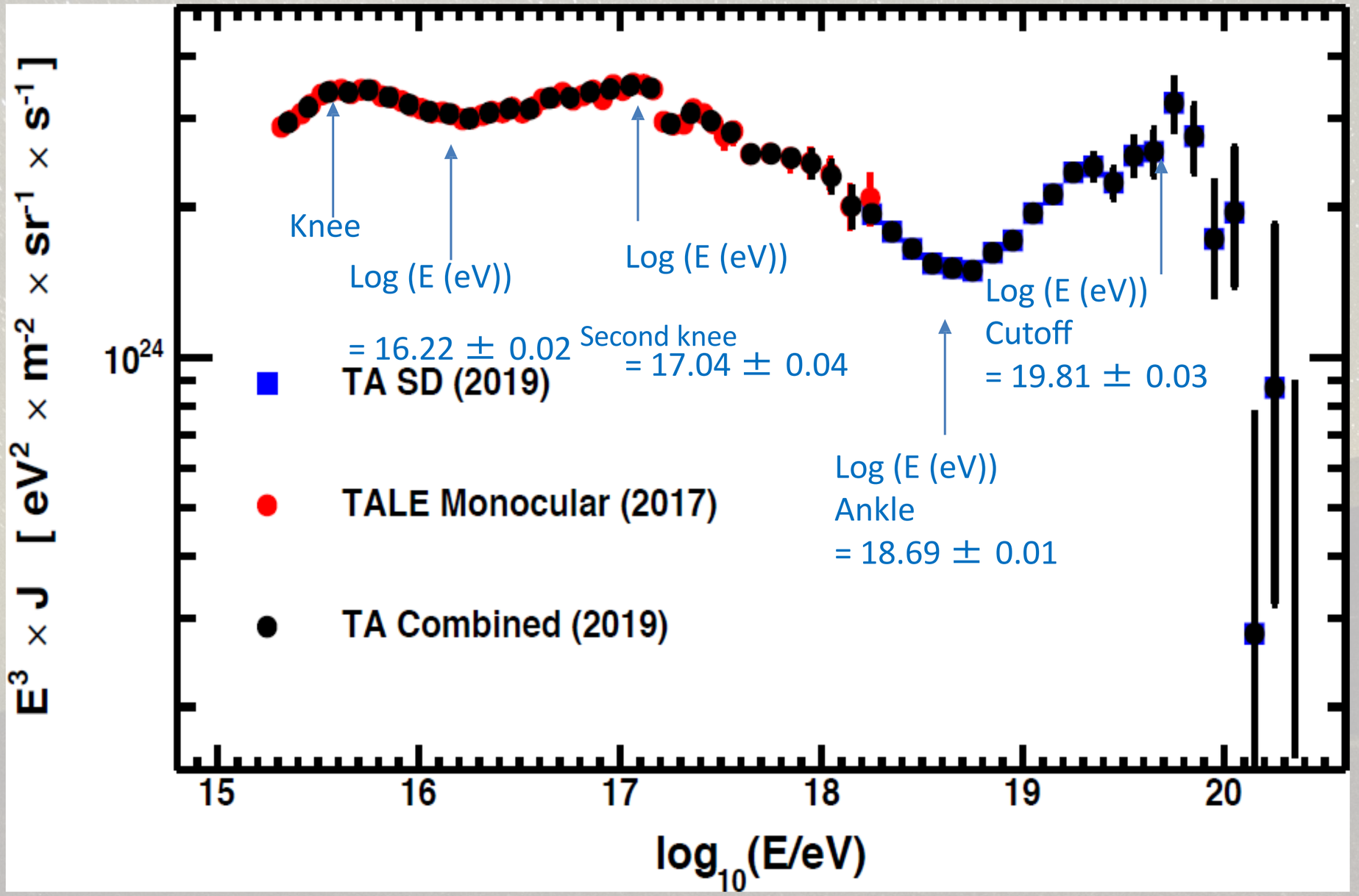

Combined TA spectrum using 22 months TALE FD monocular data + 11 years TA SD data

TA: Зависимость спектра от склонения

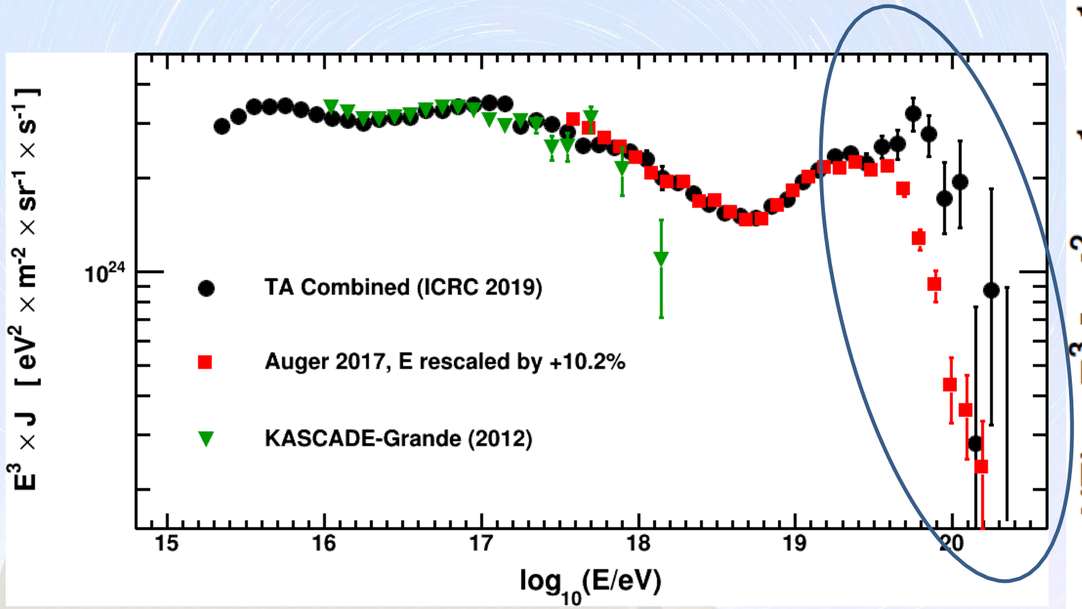

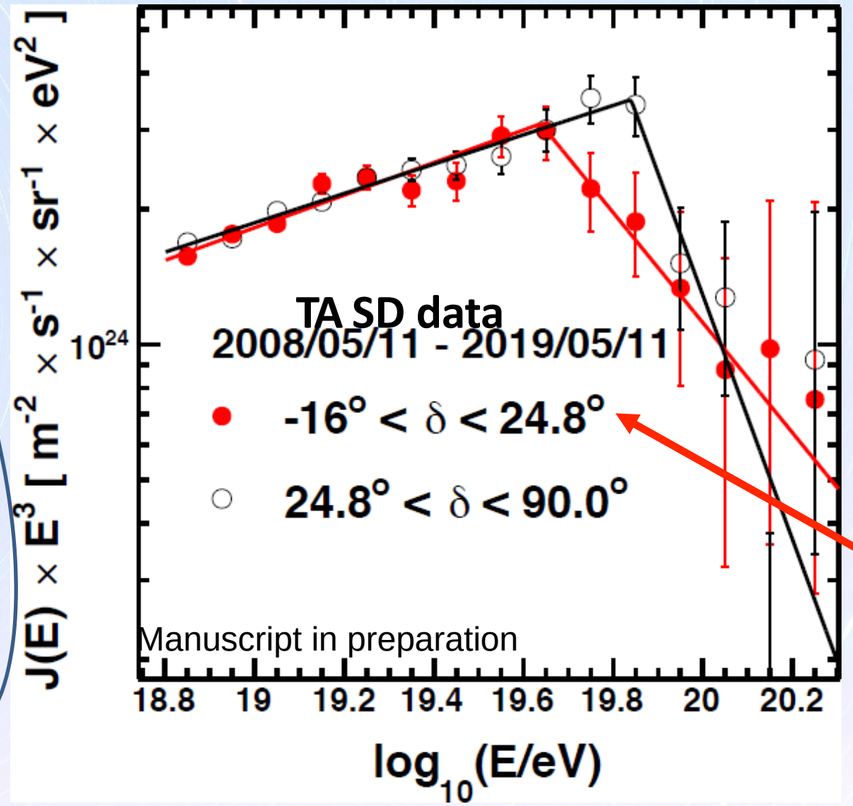

- Difference of the cutoff energies of energy spectra
  - log(E/eV) = 19.64 ± 0.04 for lower dec. band (-16° - 24.8°)
  - log(E/eV) = 19.84 ± 0.02 for higher dec. band (24.8° - 90°)
- The global significance of the difference is estimated to be 4.3σ

TA Collaboration, arXiv:1801.07820

Joint Auger + TA spectrum WG result

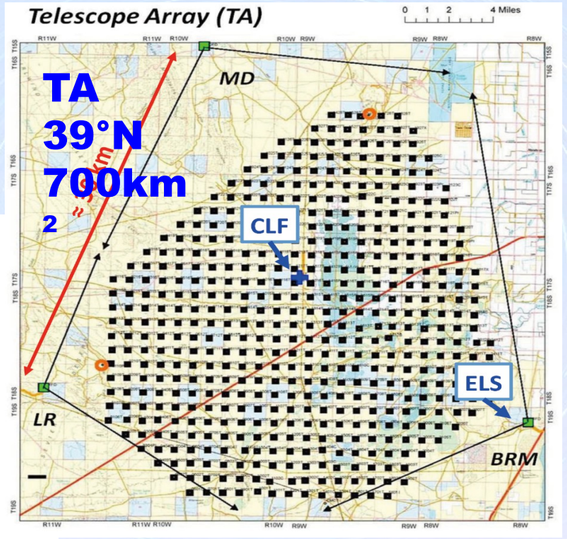

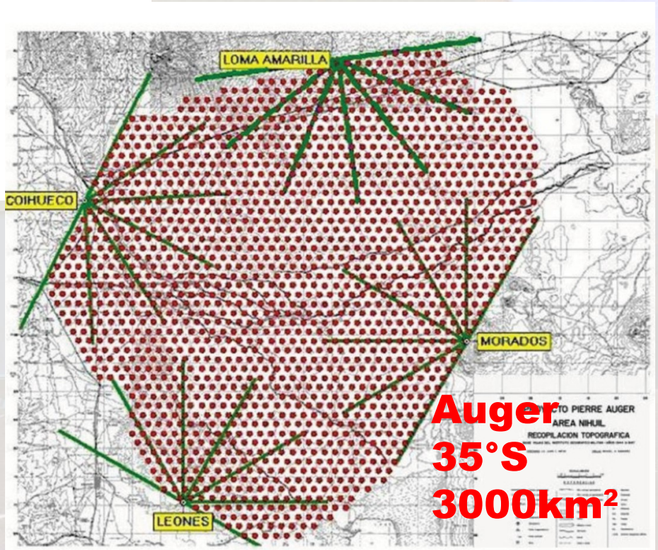

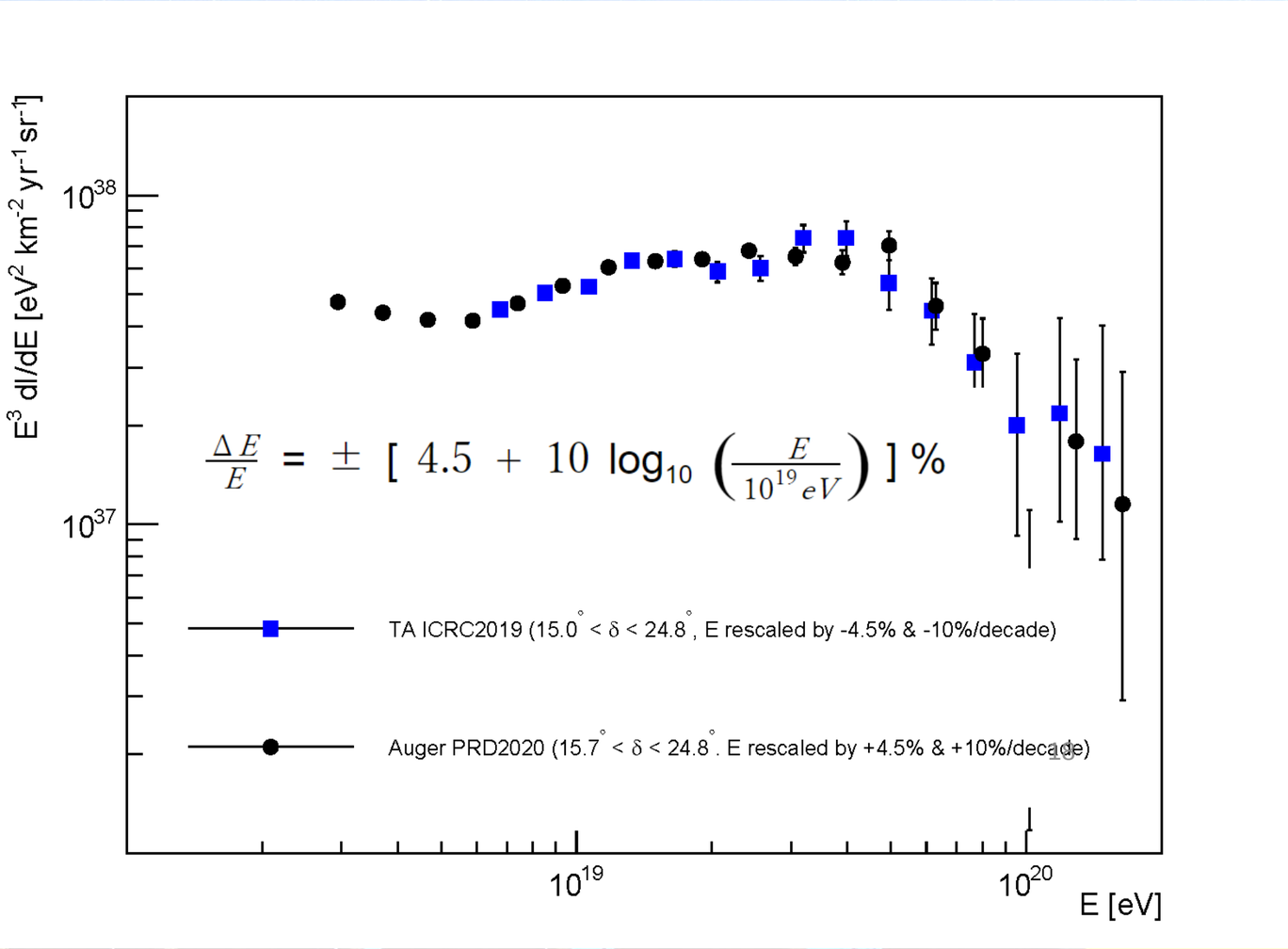

Absolute energy scale difference 9% + energy-dependent shift of ±10% per decade

Yoshiki Tsunesada, ICRC'2021

Highest Energy Event by a Surface Detector Array

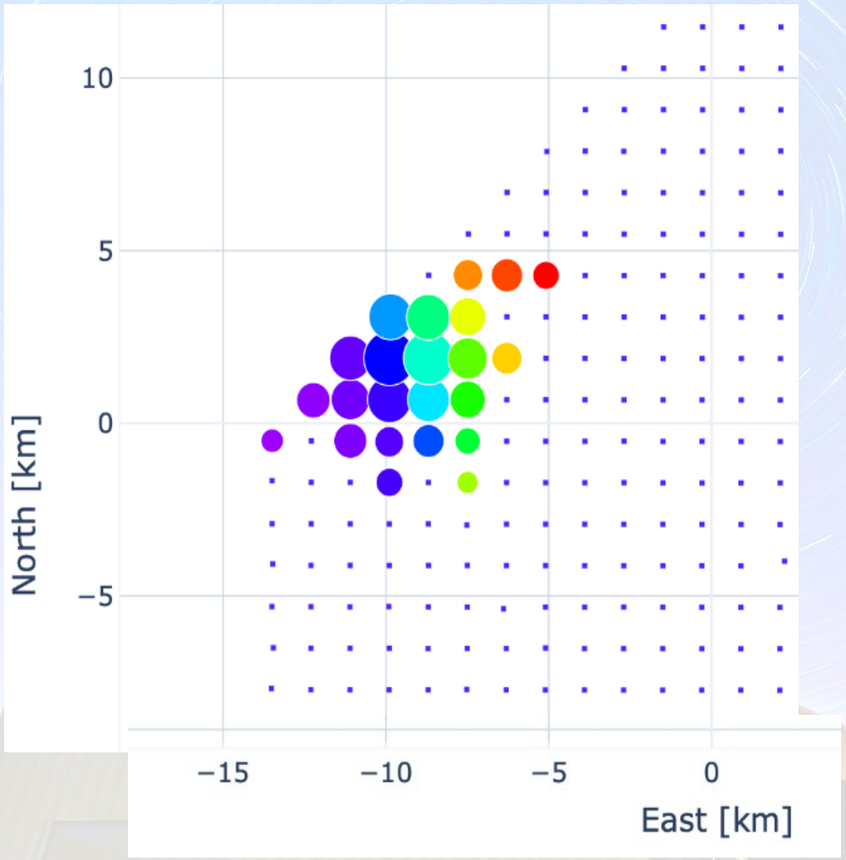

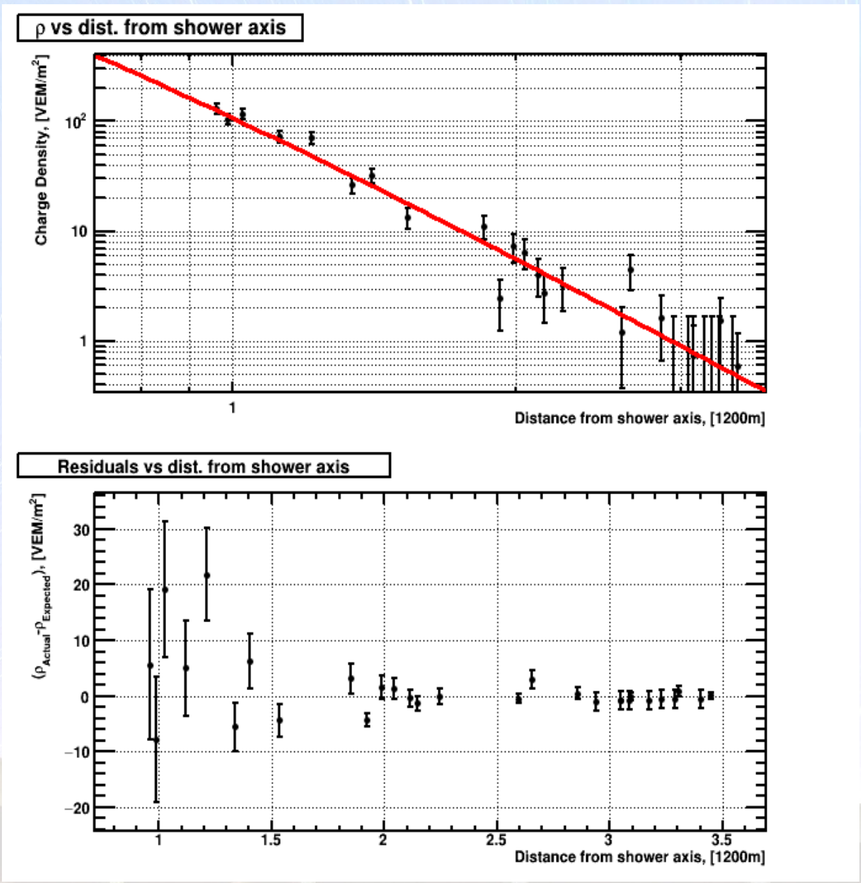

- Observed with TA SD at 10:35:56 on 27 May 2021 (UTC)
  - No FD observation
- E = **244 ± 29(stat.) ± 51(syst.) EeV**, zenith angle θ = 38.6°

Химический состав и адронные взаимодействия

20

TALE FD monocular XMAX

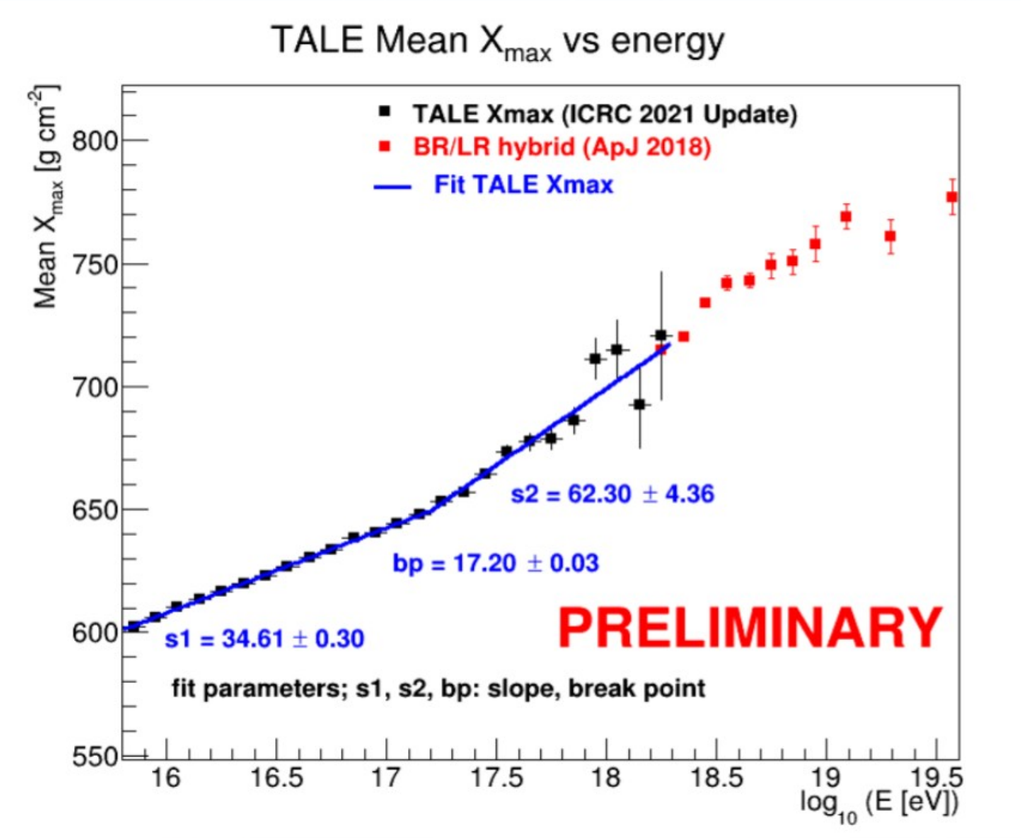

Tareq AbuZayyad, ICRC'2021

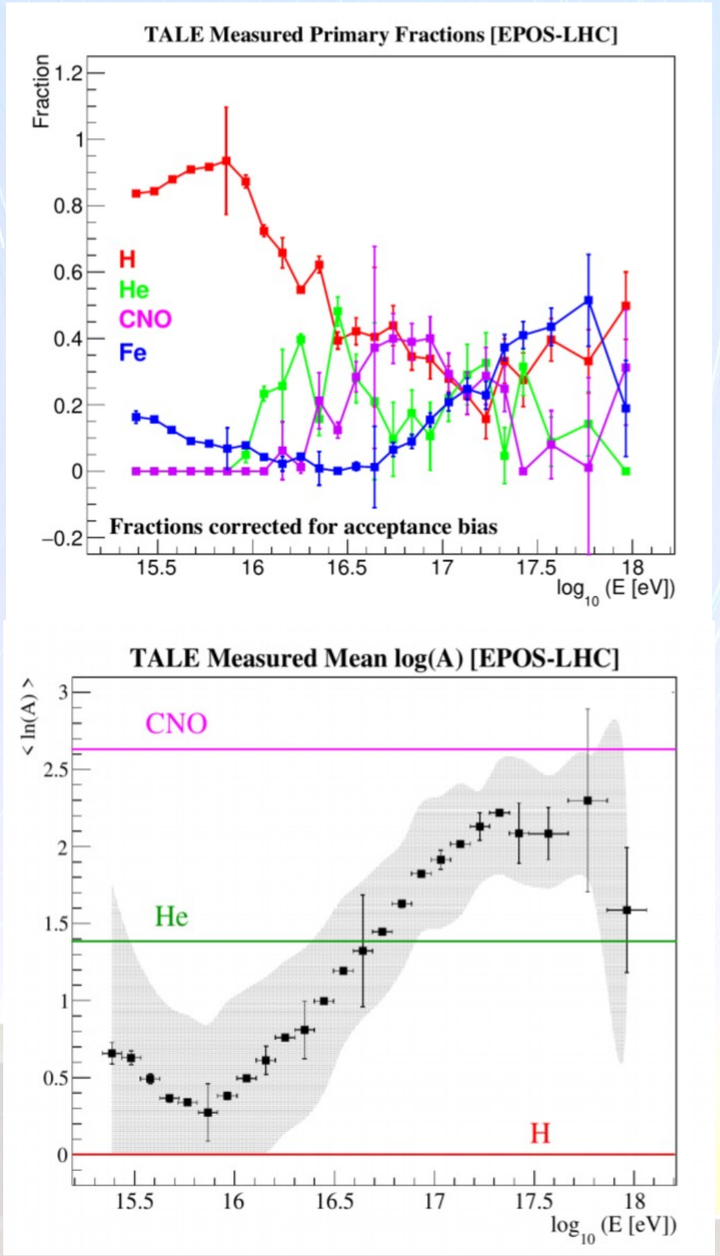

TA Collaboration ApJ 909 (2021)

A break in the elongation rate at energy $10^{17.2}$ eV

TA and TALE hybrid XMAX

TALE hybrid

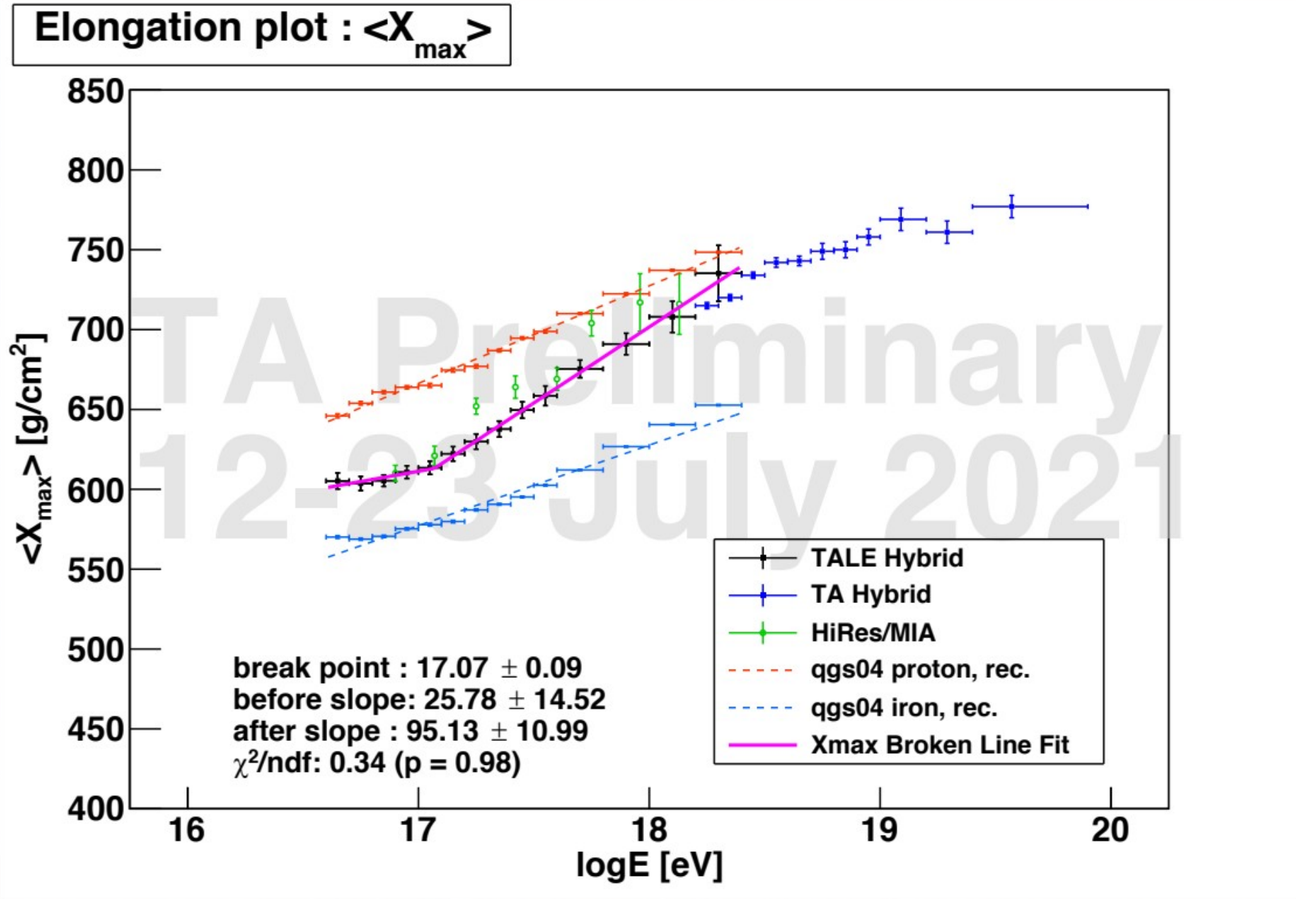

Keitaro Fujita, ICRC'2021

TA hybrid

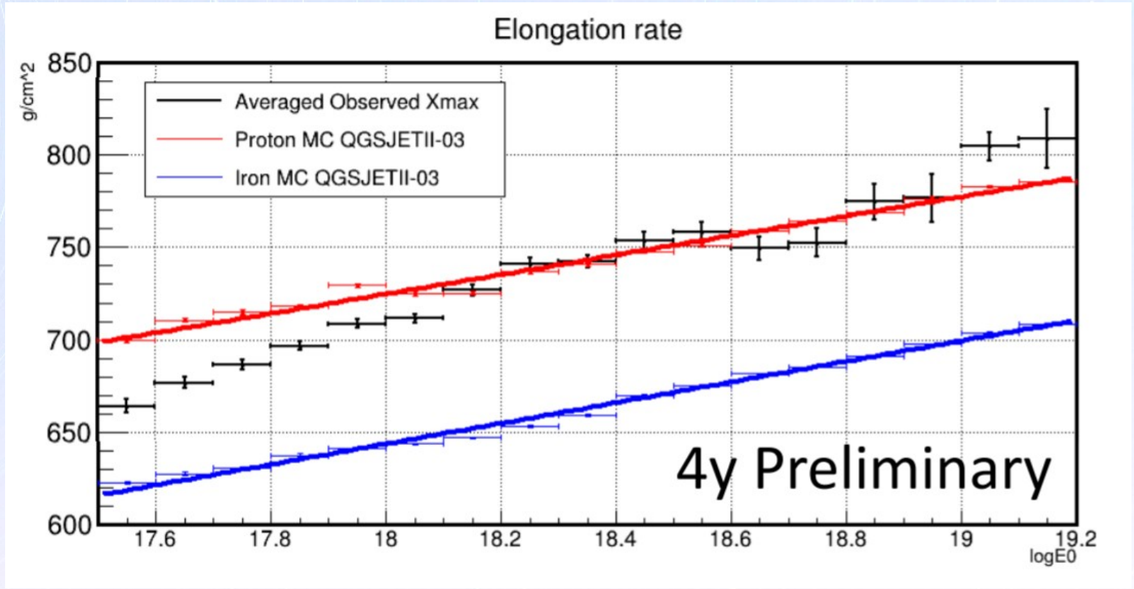

Heungsu Shin, ICRC'2021

TA SD composition

Machine learning technique based on BDT and 16 composition-sensitive observables with 12 years of TA SD data

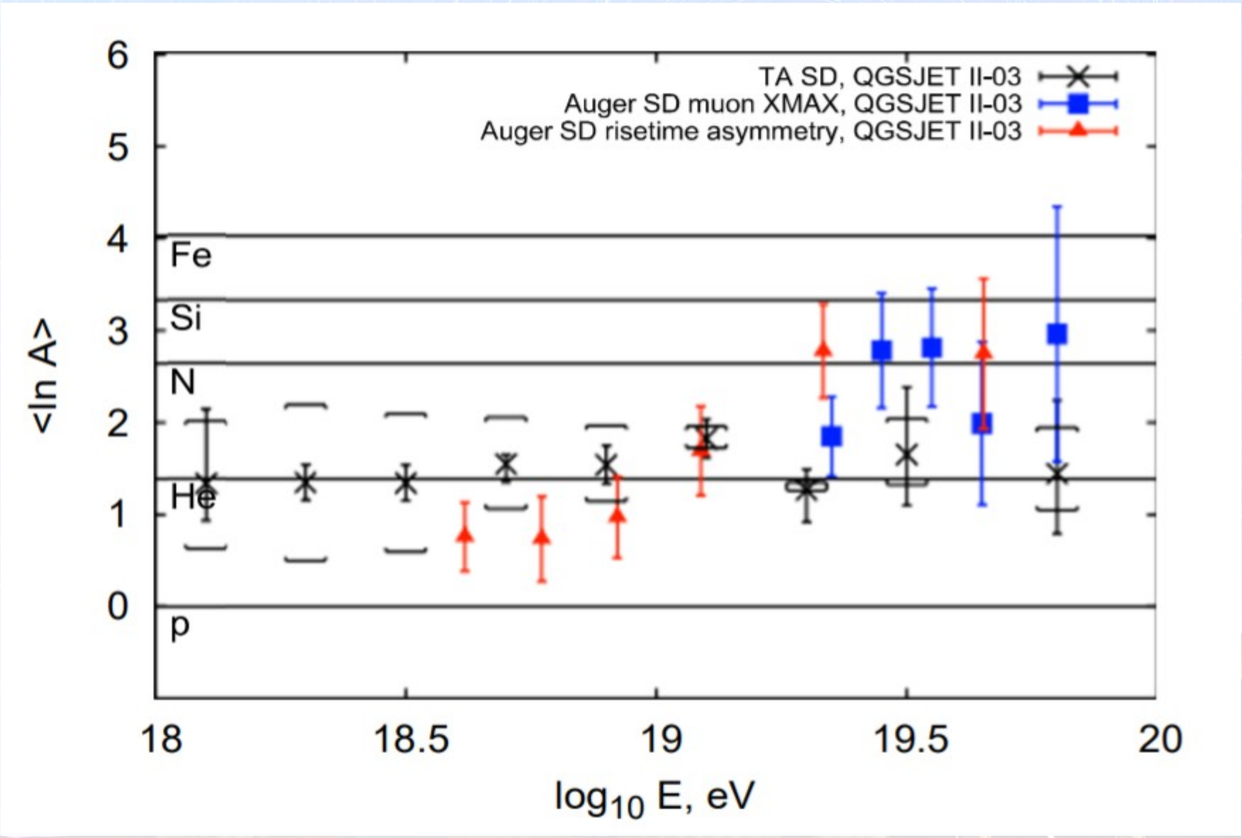

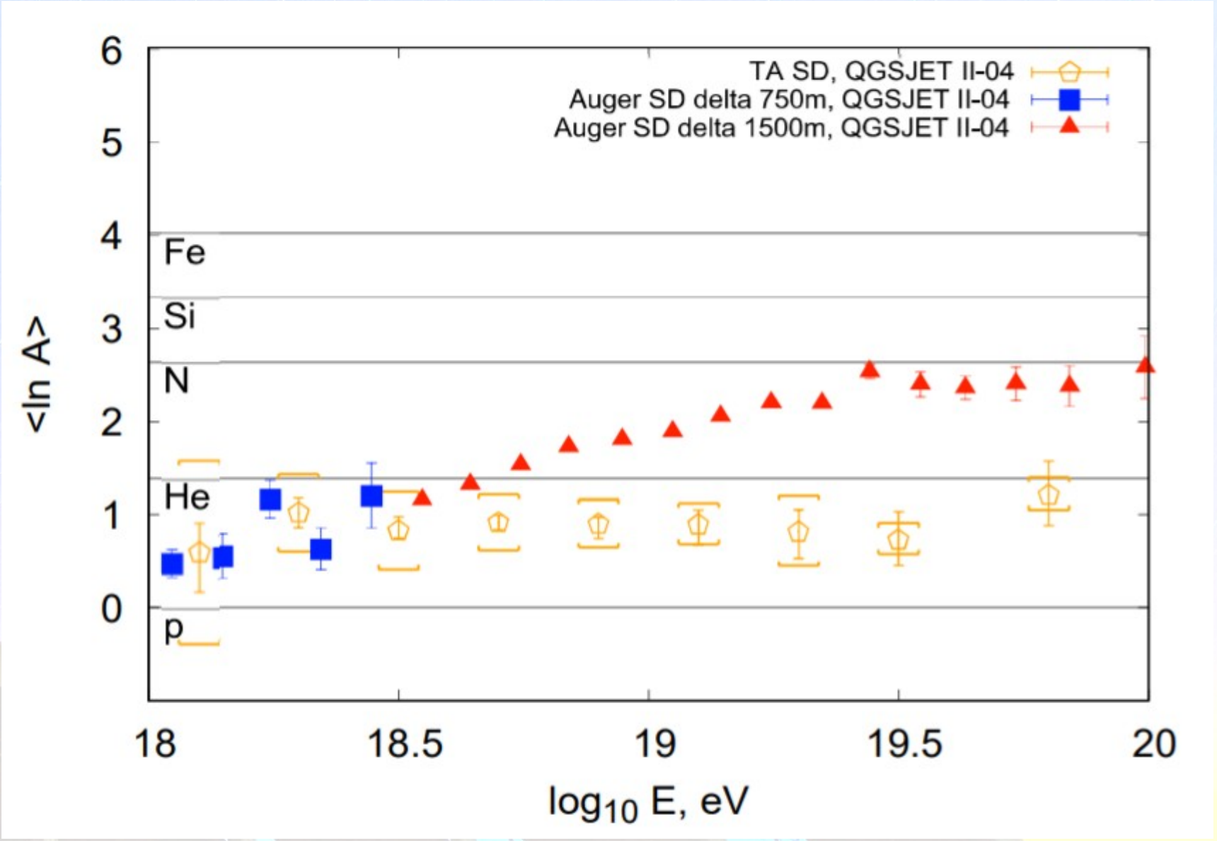

Yana Zhezher, ICRC'2021

Анализ мюонной составляющей ШАЛ

- 9 experiments: Data taken over large parameter space under very different experimental conditions!
- Muon content is expressed in terms of z-scale:

$$z = \frac{\ln(N_\mu^{\mathrm{det}}) - \ln(N_{\mu,\mathrm{p}}^{\mathrm{det}})}{\ln(N_{\mu,\mathrm{Fe}}^{\mathrm{det}}) - \ln(N_{\mu,\mathrm{p}}^{\mathrm{det}})} \quad , \quad z = 0\text{: proton, } z = 1\text{: iron}$$

  - N_μ^{det}: muon content measured in the detector
  - $N_{\mu,\mathrm{p}}^{\mathrm{det}}$, $N_{\mu,\mathrm{Fe}}^{\mathrm{det}}$: muon content in simulated EAS (proton/iron) at the detector

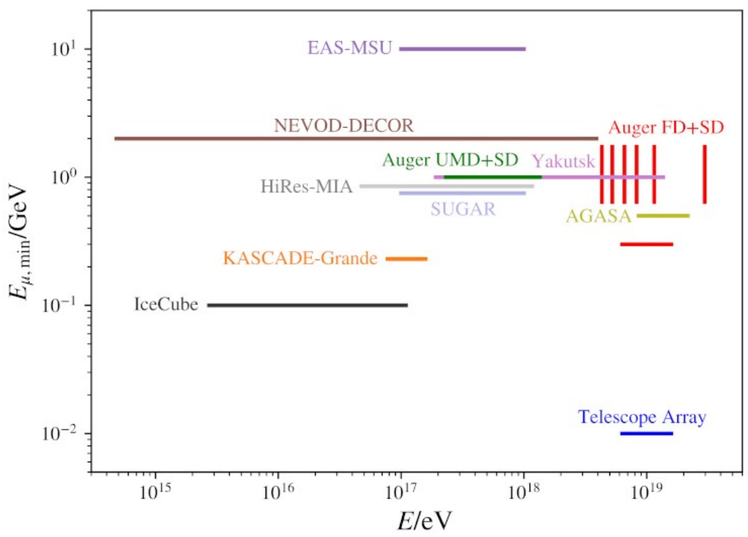

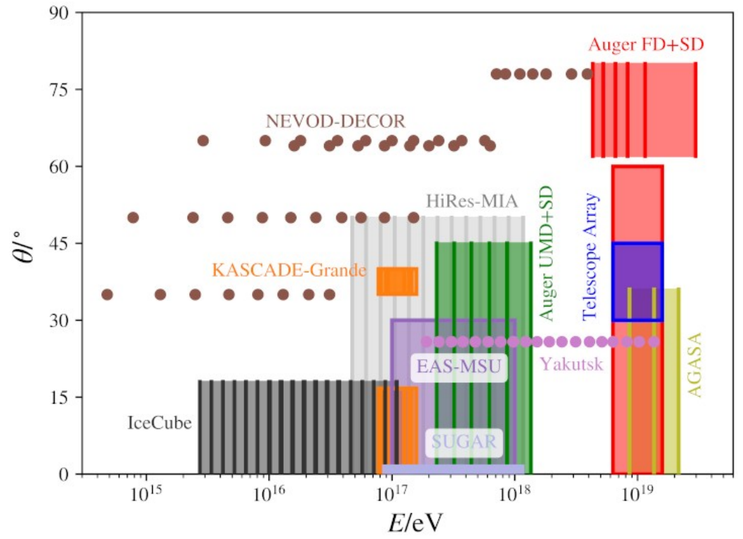

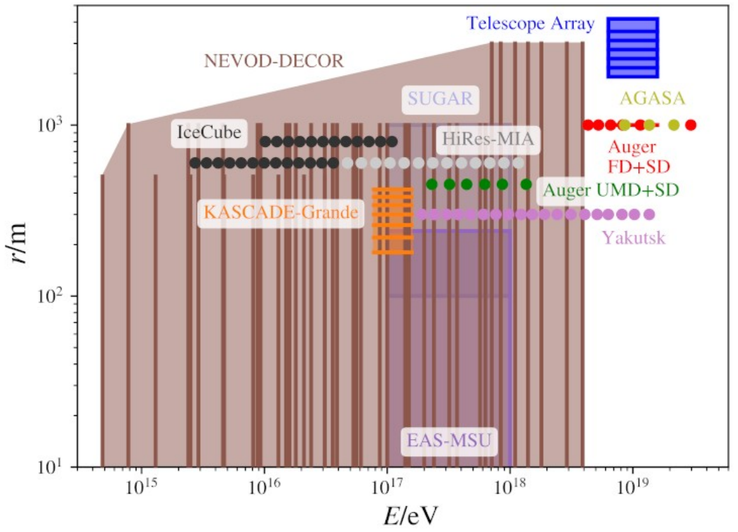

Dennis Soldin, UHECR'2022

Проблема мюонного избытка

- Muon lateral density in EAS after cross-calibration of the energy-scales

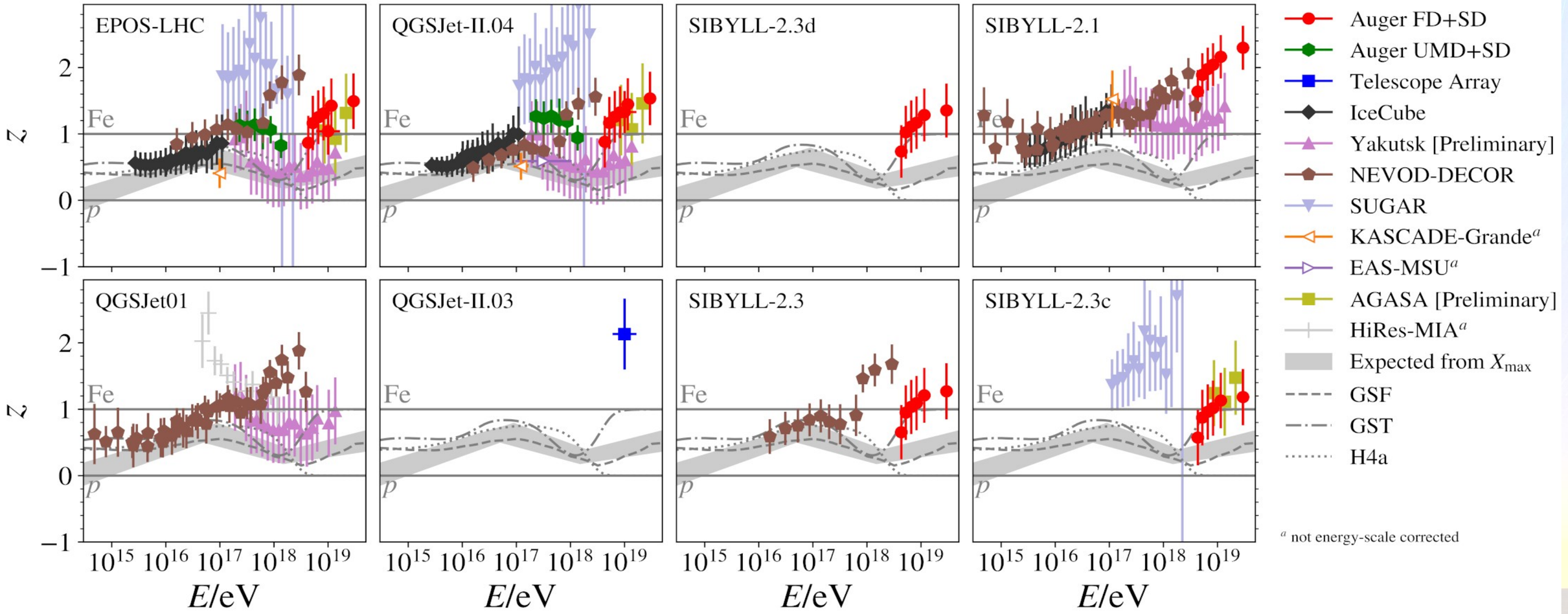

Dennis Soldin, UHECR'2022

TA proton-air cross-section

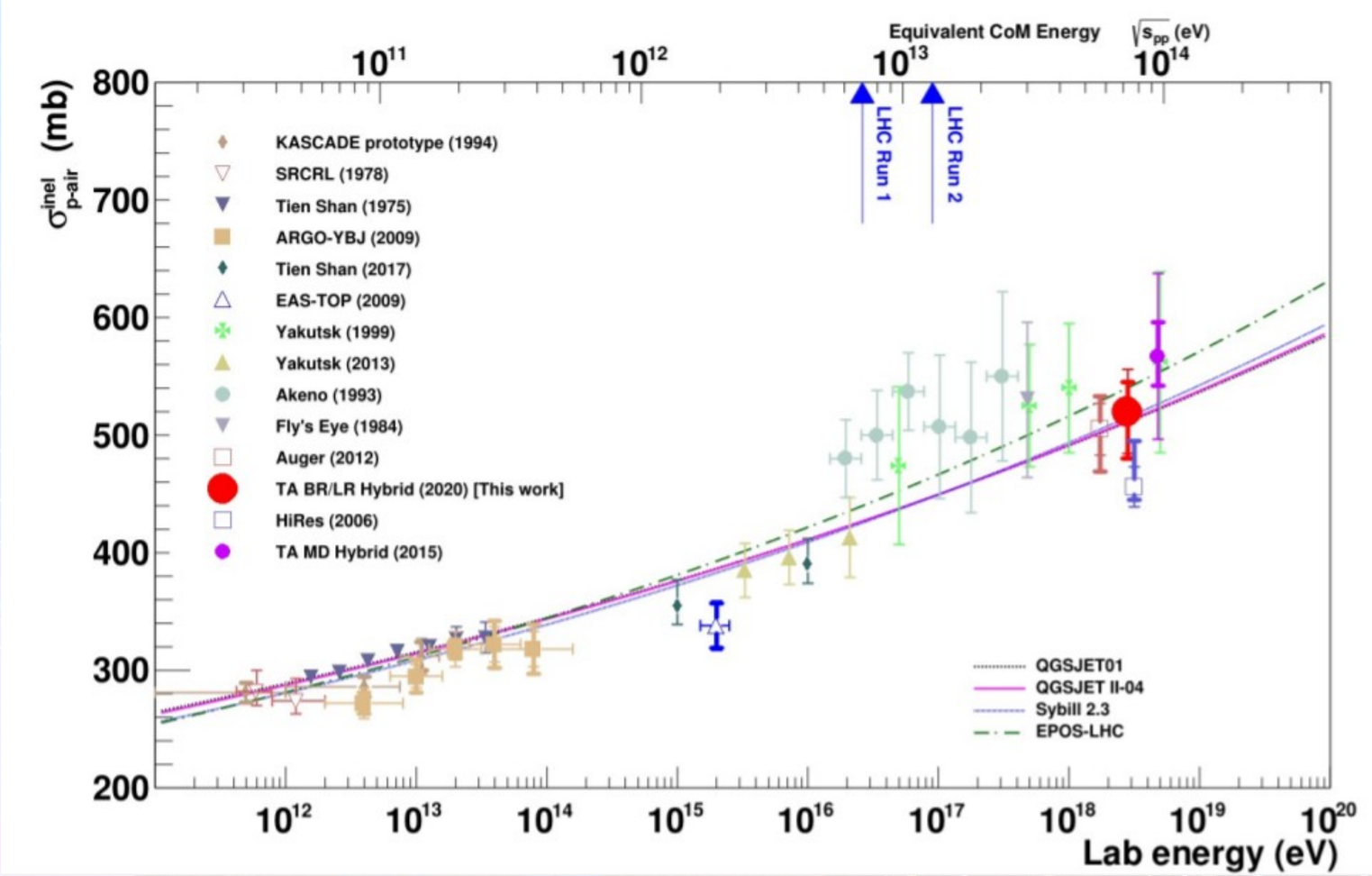

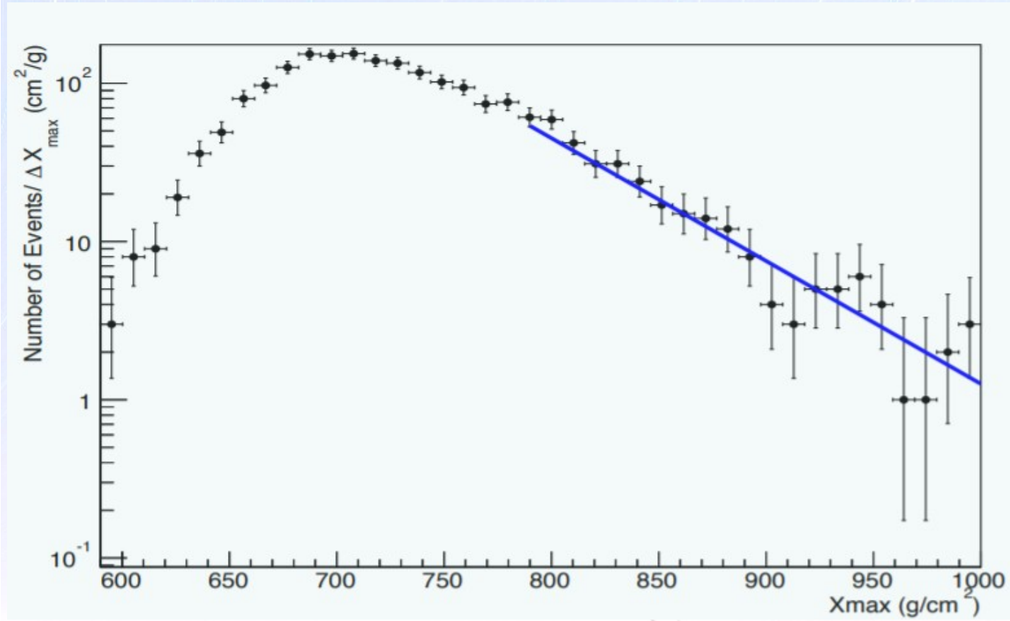

Measuring XMAX attenuation length in hybrid mode.

TA Collaboration, Phys. Rev. D 102, 062004

Поиск фотонов ультравысоких энергий

Photon-induced showers:

- develop deeper in the atmosphere ⇒ arrive younger
- contain less muons ⇒ SD waveforms are less compressed

We use the neural-network classifier trained on both the

- **time-resolved waveforms**
- and derived features: front curvature, Area-over-peak, number of FADC signal peaks, $\chi^2/d.o.f.$, S_b

p-γ classifier based on neural network

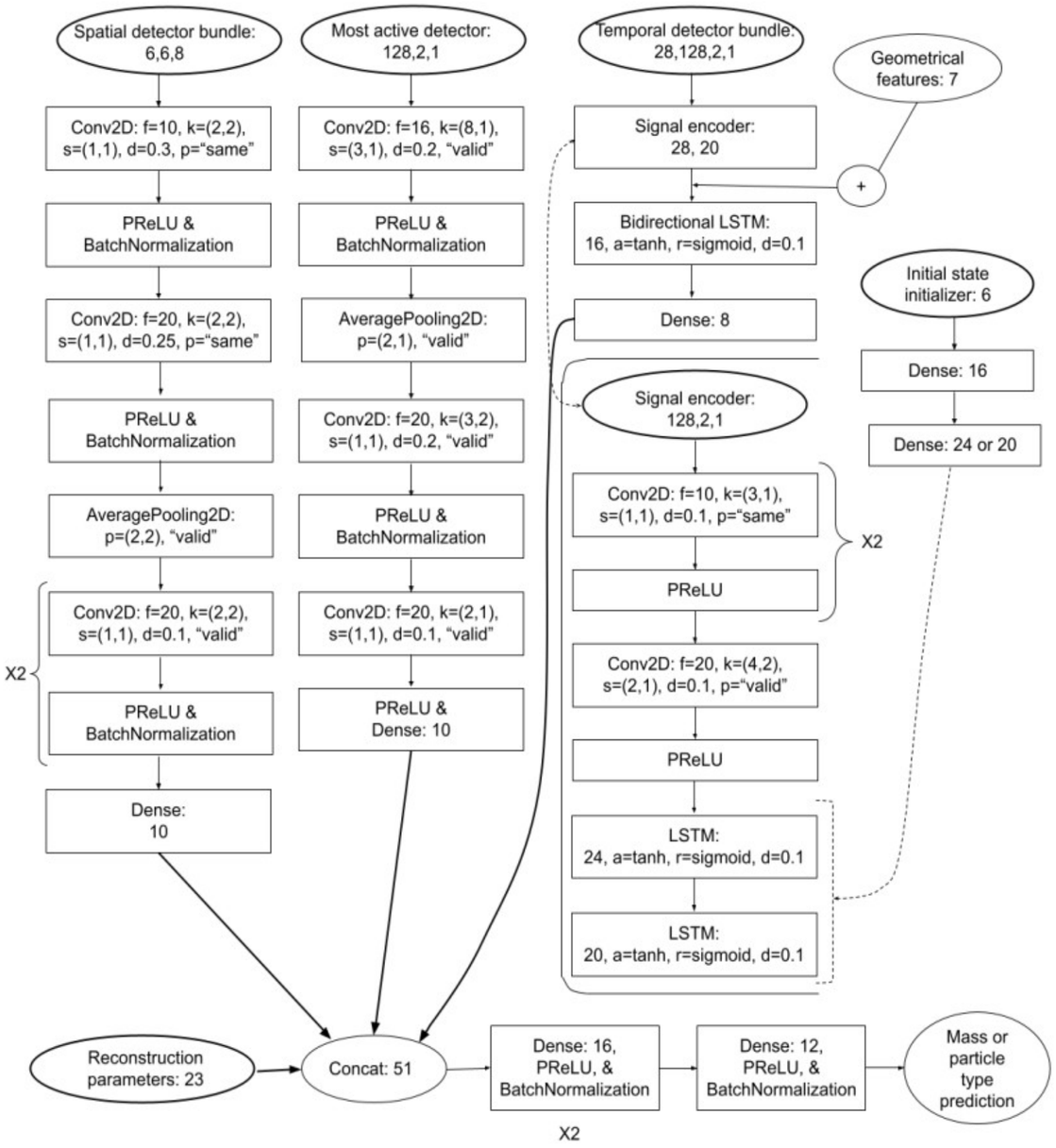

Input:

- incidence time and integral signal for 6x6 SD stations
- time-resolved signals for all triggered stations ordered by the front arrival time
- composition-sensitive event features

TA, Phys.Rev.D 99 (2019) 02200

Output:

- The value $\xi \in [0, 1]$ for an event. ξ is close to 0 for proton-induced showers and to 1 for γ-induced.

p-γ classifier: list of event features

1. Zenith angle, θ;
2. Signal density at 800 m from the shower core, S_{800};
3. Linsley front curvature parameter, a;
4. Area-over-peak (AoP) of the signal at 1200 m;

Pierre Auger Collaboration, Phys.Rev.Lett. 100 (2008) 211101

5. AoP LDF slope parameter;
6. Number of detectors hit;
7. N. of detectors excluded from the fit of the shower front;
8. $\chi^2/d.o.f.$;
9. $S_b = \sum S_i \times r_i^b$ parameter for $b = 2.5, 3.0, 3.5, 4.0$ and $b = 4.5$;

Ros, Supanitsky, Medina-Tanco et al. Astropart.Phys. 47 (2013) 10

10. The sum of signals of all detectors of the event;
11. Asymmetry of signal at upper and lower layers of detectors;
12. Total n. of peaks within all FADC traces;
13. N. of peaks for the detector with the largest signal;

14-15. N. of peaks present in the upper layer and not in lower (and vice versa);

Photon search with p-γ classifier

- The p-γ classifier is trained with two Monte-Carlo sets:
  - γ-induced events (Signal)
  - proton-induced events (Background)

- The output of the classifier for each event is a number $\xi \in [0:1]$: 1 – pure signal (γ), 0 – pure background (p).

- We call “photon-candidates” events with $\xi > \xi_{cut}$.

- The optimal value of ξ_{cut} is obtained by the requirement of the strongest sensitivity in case null-hypothesis is valid, i.e. all events are protons.

Photon search: data and Monte-Carlo sets

- Data collected by TA surface detector for the 11 years:
  2008-05-11 – 2019-05-10
- p and γ Monte-Carlo sets with CORSIKA and dethinning

Stokes et al, Astropart.Phys.35:759,2012

Cuts for both data and MC:

- 7 or more detectors triggered
- core distance to array boundary is larger than 1200m
- $\chi^2/\text{d.o.f.} < 5$
- $\theta < 55°$
- $E_\gamma > 10^{19.0}$ eV (E_γ is estimated with photon Monte-Carlo)
  - or $E_\gamma > 10^{18.5}$ eV for training Monte-Carlo sets

11327 events after cuts

MC set is split into 3 parts: (I) 80% of events, for training the classifier, (II) for testing and cut optimization, (III) for exposure estimate.

Distribution of classifier result (ξ) for data and MC

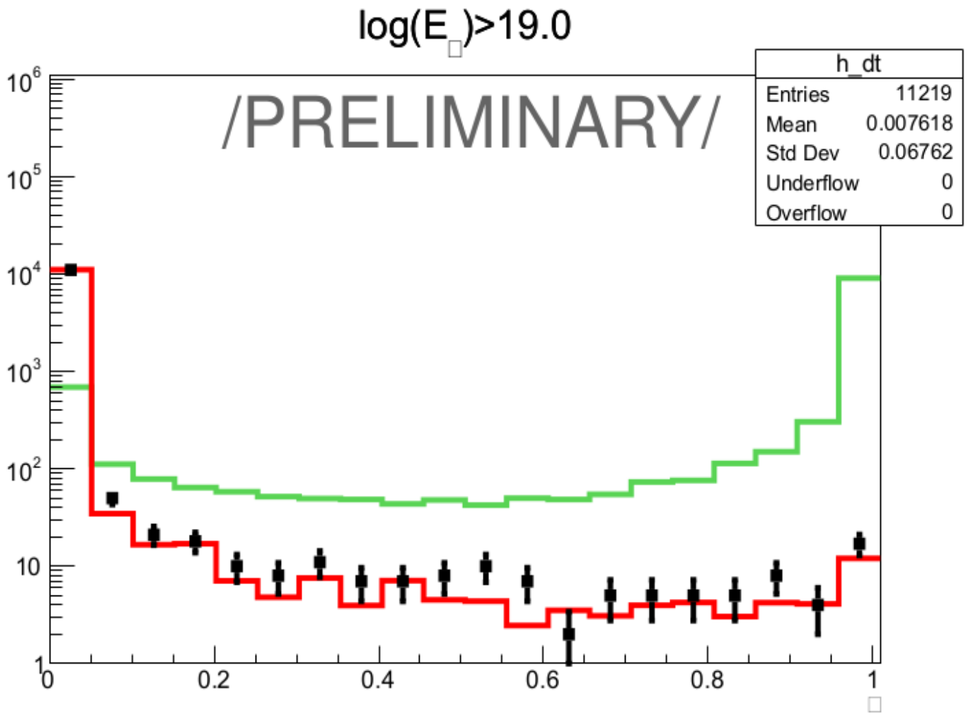

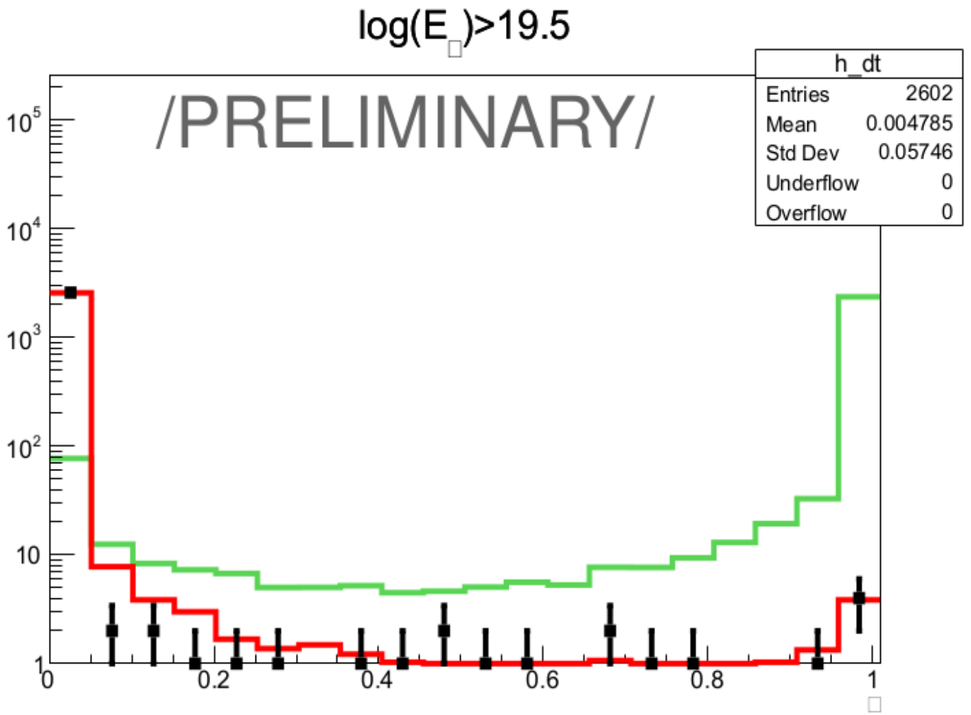

data photon MC proton MC

Efficient separation of proton and photon-induced events.

Effective exposure

- Geometric exposure for $\theta \in (0°, 55°)$: **13221 km^2 sr yr**

- Effective exposure is estimated using photon MC assuming E^{-2} primary spectrum

E_0	quality cuts	$\xi > \xi_{cut}$	A_{eff} km^2 sr yr
$10^{19.0}$	43.7%	**59.4%**	**3428**
$10^{19.5}$	52.0%	**80.7%**	**5546**
$10^{20.0}$	64.3%	**92.7%**	**7875**

- Efficiency of photon candidate selection ($\xi > \xi_{cut}$) has substantially grown compared to the previous analysis with BDT classifier – 16.2%, 37.2% and 52.3% for $\log_{10} E_0 = 19.0, 19.5$ and 20.0, correspondingly.

TA Collaboration, Astroparticle Physics 110 (2019) 8

Photon candidate events for $E_0 > 10^{19.0}$ eV

energy cut	event date and time	comment
$E_0 > 10^{19.0}$ eV	2010-10-04 16:58:42	
	2011-07-27 08:06:15	
	2011-09-16 19:40:56	
	2012-05-01 00:59:15	
	2012-07-06 01:49:11	
	2012-09-07 01:55:45	
	2013-08-27 22:38:37	
	2014-07-31 21:19:19	
	2014-08-14 09:46:58	
	2014-08-23 02:39:15	
	2014-09-27 07:54:35	
	2015-07-19 01:03:04	
	2017-09-12 18:32:59	
	2018-08-02 15:25:51	
	2018-10-03 04:03:48	
	2019-04-30 22:43:17	

Photon candidate events for $E_0 > 10^{19.0}$ eV

energy cut	event date and time	comment
$E_0 > 10^{19.0}$ eV	2010-10-04 16:58:42	**TGF candidate event**
	2011-07-27 08:06:15	**TGF candidate event**
	2011-09-16 19:40:56	**TGF candidate event**
	2012-05-01 00:59:15	
	2012-07-06 01:49:11	**TGF candidate event**
	2012-09-07 01:55:45	**TGF candidate event**
	2013-08-27 22:38:37	**TGF candidate event**
	2014-07-31 21:19:19	**TGF candidate event**
	2014-08-14 09:46:58	
	2014-08-23 02:39:15	**TGF candidate event**
	2014-09-27 07:54:35	**TGF candidate event**
	2015-07-19 01:03:04	**TGF candidate event**
	2017-09-12 18:32:59	**TGF candidate event**
	2018-08-02 15:25:51	**TGF candidate event**
	2018-10-03 04:03:48	**TGF candidate event**
	2019-04-30 22:43:17	**TGF candidate event**

Terrestrial Gamma-Ray Flashes candidate events are time correlated with the lightnings registered by National Lightning Detection Network.

TA collaboration, JGR Atmospheres (2020)
J. Remington, talk 828, this conference

- 2 photon-candidate events observed
- 0.8 events expected from proton MC

Results: photon flux limits

E_0, eV	$10^{19.0}$	$10^{19.5}$	$10^{20.0}$
γ candidates	~~16~~ 2	~~11~~ 1	~~5~~ 0
$\bar{n}$ <	6.72	5.14	3.09
A_{eff}	3428	5546	7875
F_γ <	2.0×10^{-3}	9.3×10^{-4}	3.9×10^{-4}

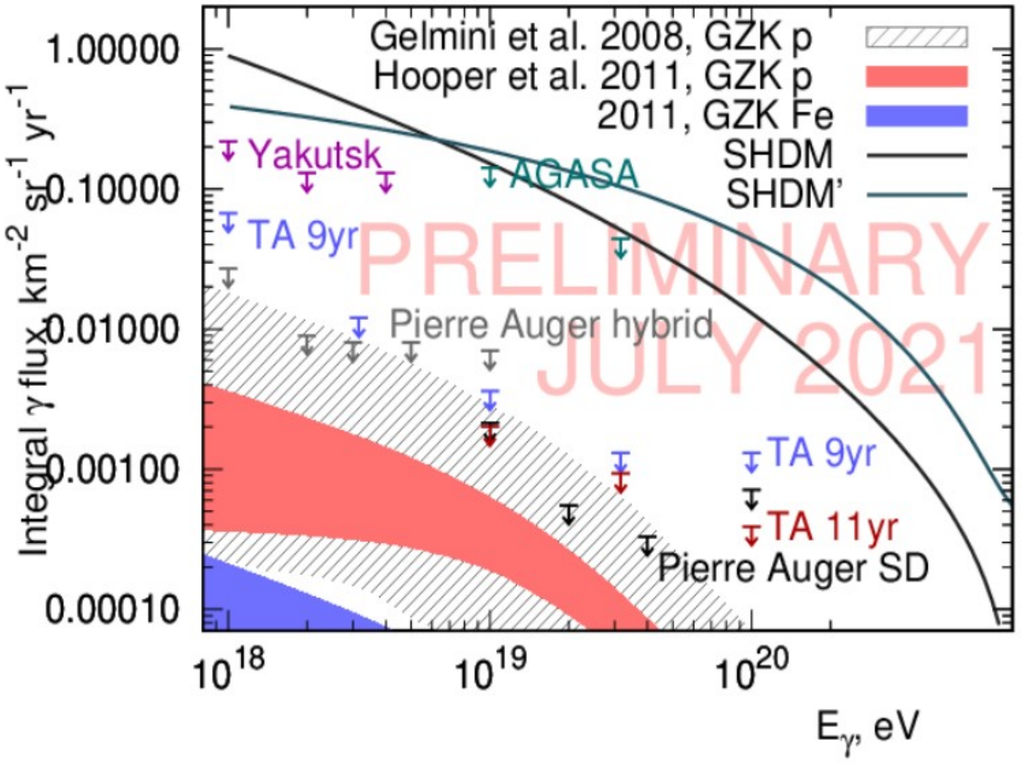

Поиск нейтрино ультравысоких энергий

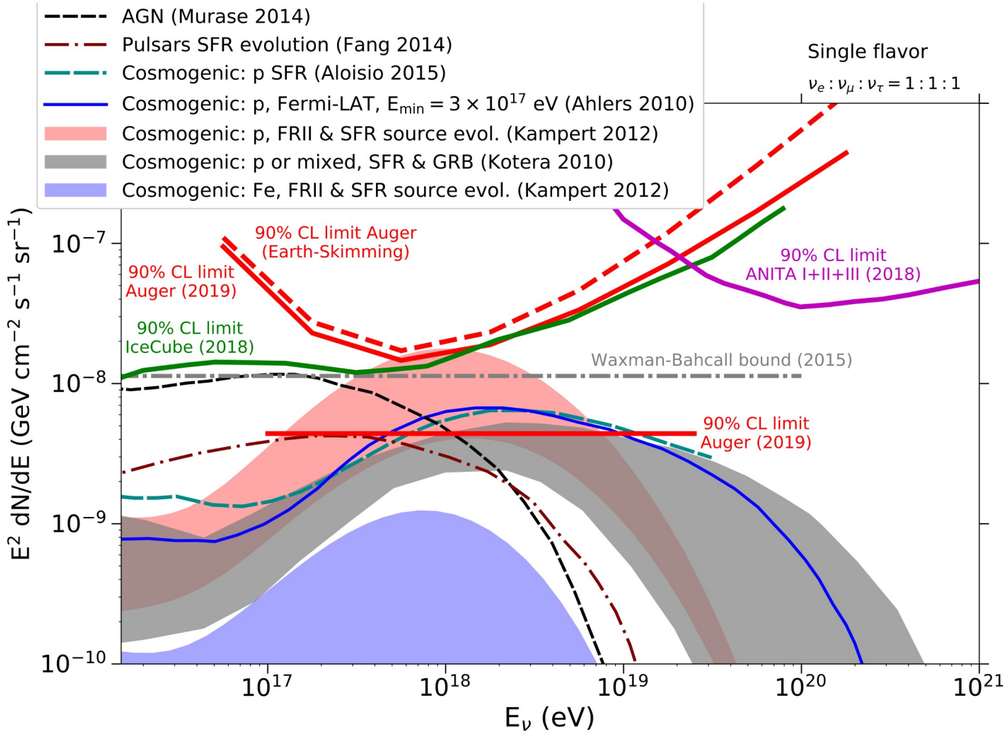

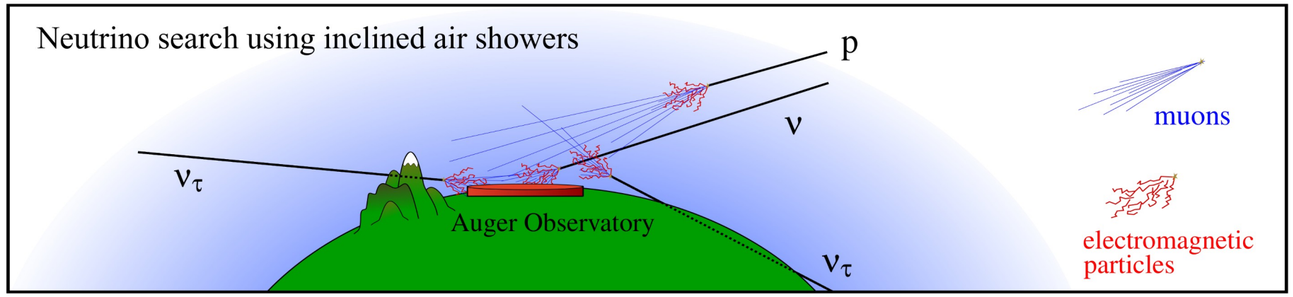

(JCAP 10 (2019) 022, JCAP 11 (2019) 004)

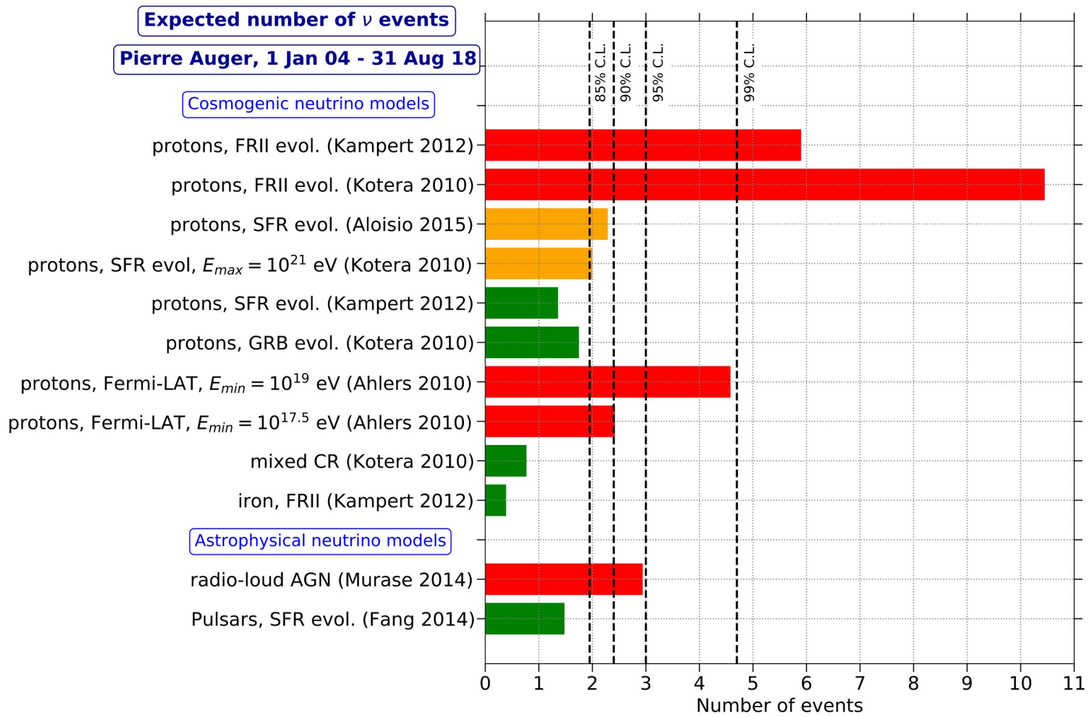

Aperture comparable to IceCube if direction of source is favorable

Multi-messenger: searches for neutrinos in coincidence with GW events

Phase II: lowering of detection threshold (new electronics)

Anisotropy

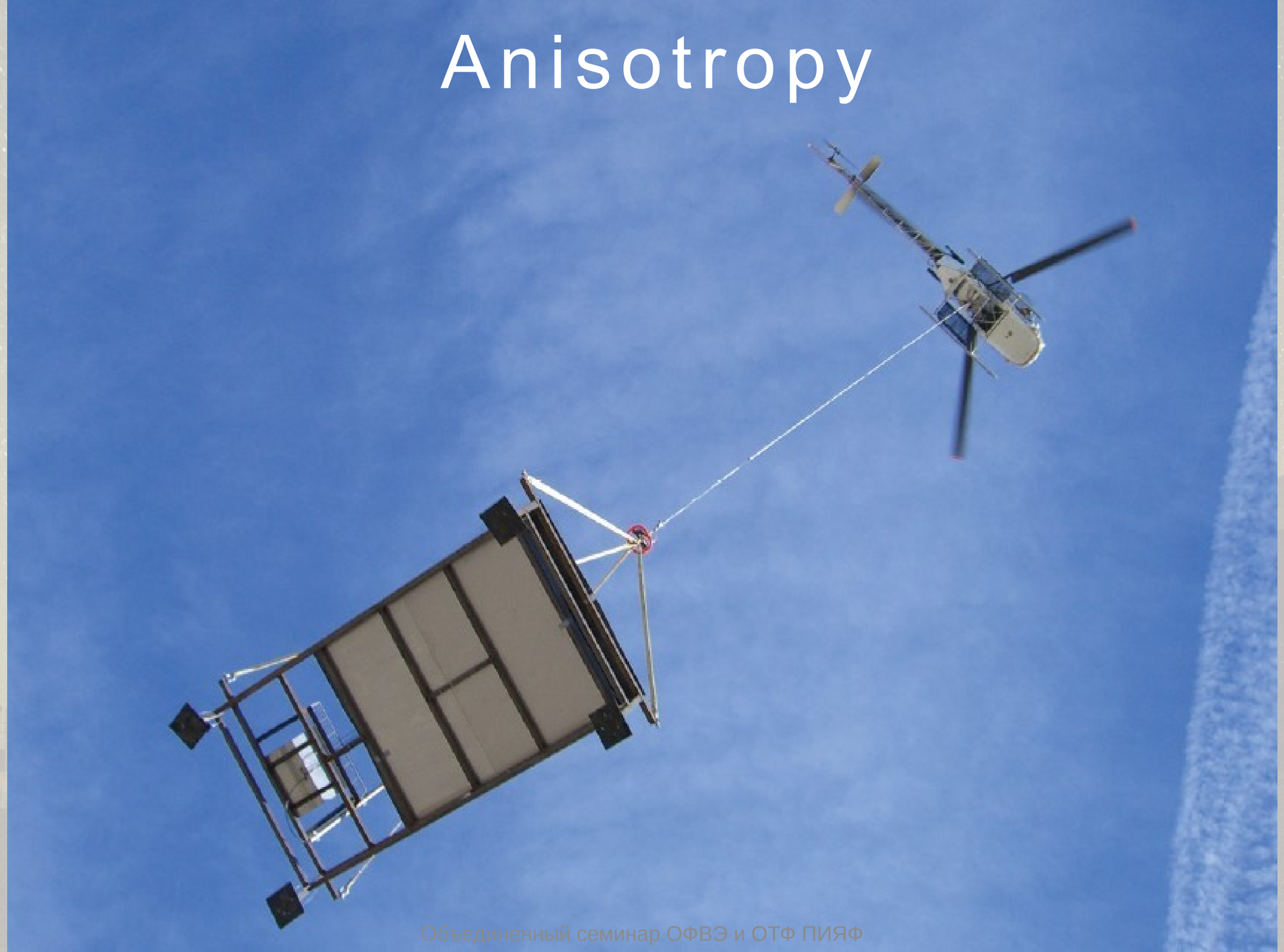

Возможные источники КЛУВЭ

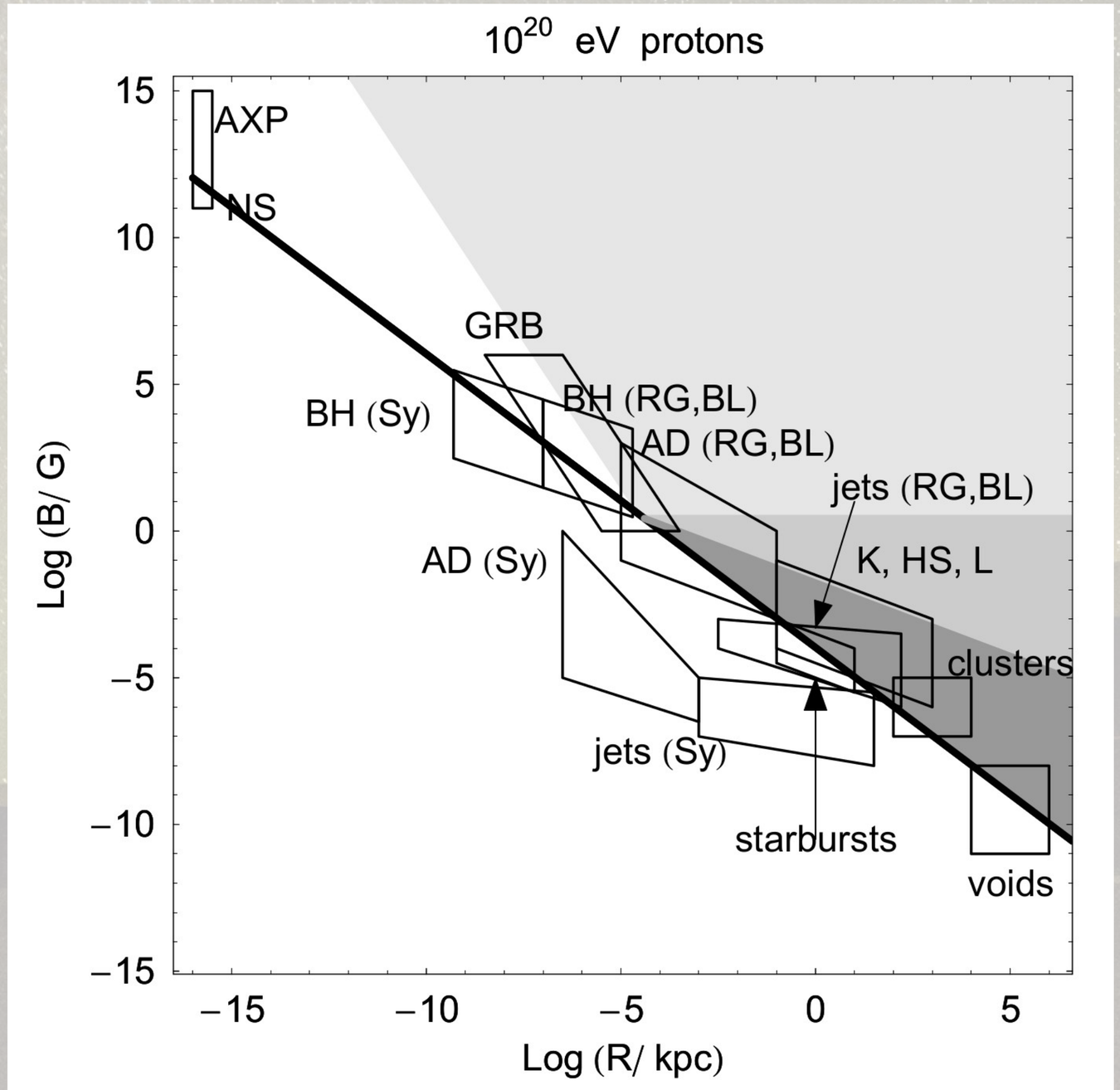

Птицына, Троицкий,
УФН 53 (2020) 691

Сколько источников КЛУВЭ?

- Пусть мы видим N_{tot} событий
- Наблюдается N_{cl} кластеров на величие углового разрешения (отклонения в магнитных полях)
- Если кластеров мало, значит каждый источник в среднем производит в нашей выборке заметно меньше одного фотона
- Ограничение на минимальное число источников в видимой области (ГЗК-сфера) $\sim \pi N_{tot}^3/3N_{cl}^2$

  Дубовский, Тиняков, Ткачев, Phys.Rev.Lett. 85 (2000) 1154-1157
- По данным Auger для $E > 50$ ЭэВ, получаем $n > 10^{-4}$ Мрс$^{-3}$ (если источники производят протоны)

  Калашев, Птицына, Троицкий, Phys.Rev. D86 (2012) 063005

Вопреки ожиданиям, источники не найдены

Как нам представляется, к 2001 году или во всяком случае к 2012 году можно ожидать выяснения почти всех вопросов, сформулированных в конце предыдущего параграфа.

В.Л. Гинзбург, Астрофизика космических лучей, 1990 г.

(Примечание: речь об источниках КЛУВЭ)

Поиск диполя и квадруполя

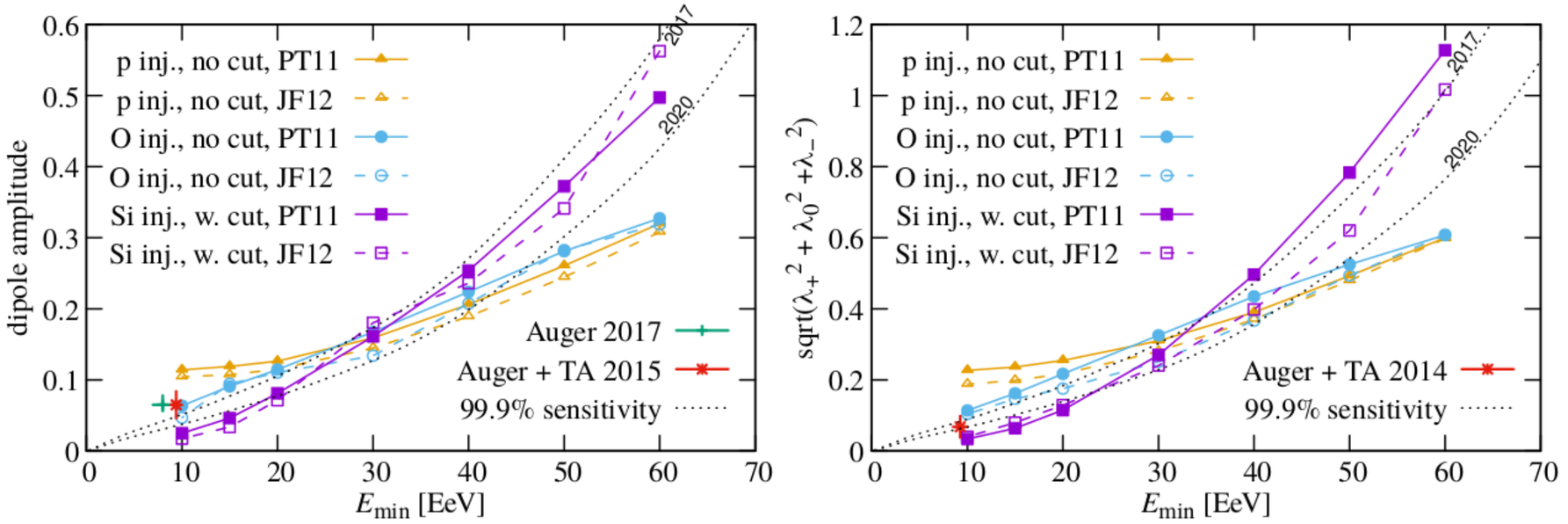

di Matteo, Tinyakov, MNRAS 476 (2018) 715

- В модели источников, повторяющей LSS, предсказан рост диполя и квадруполя с энергией
- Данные Оже по диполю согласуются с предсказанием
- Квадруполь не обнаружен: аргумент против чисто протонного состава

Поиск диполя и квадруполя

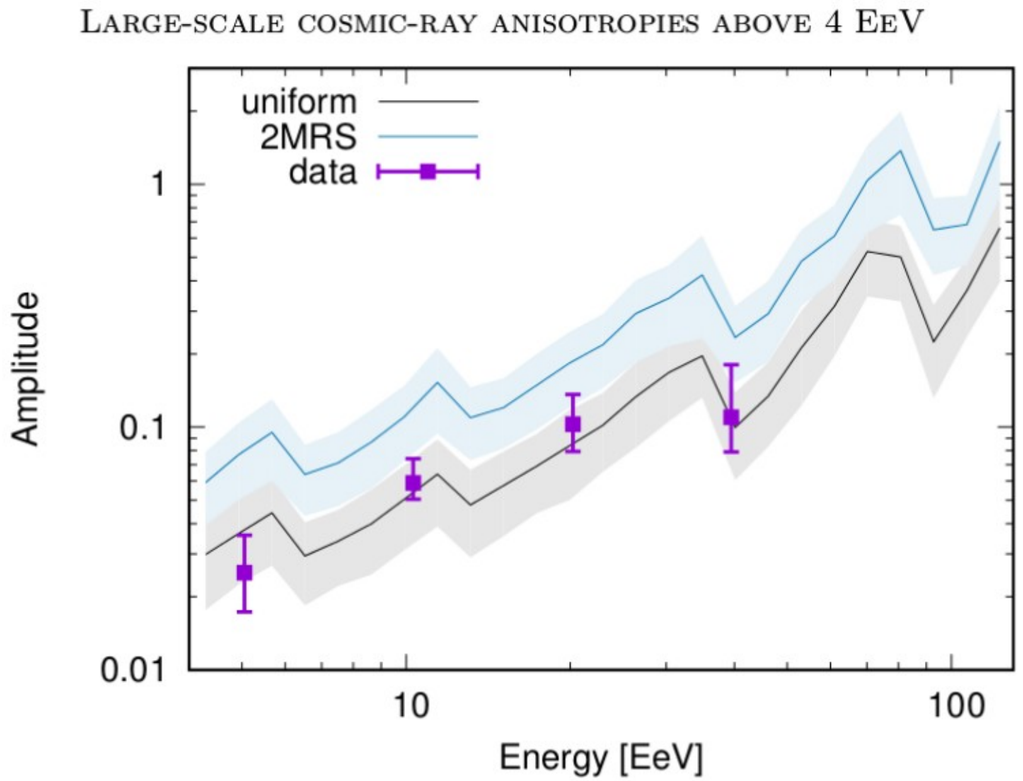

Auger collaboration, ApJ 868 (2018) 4

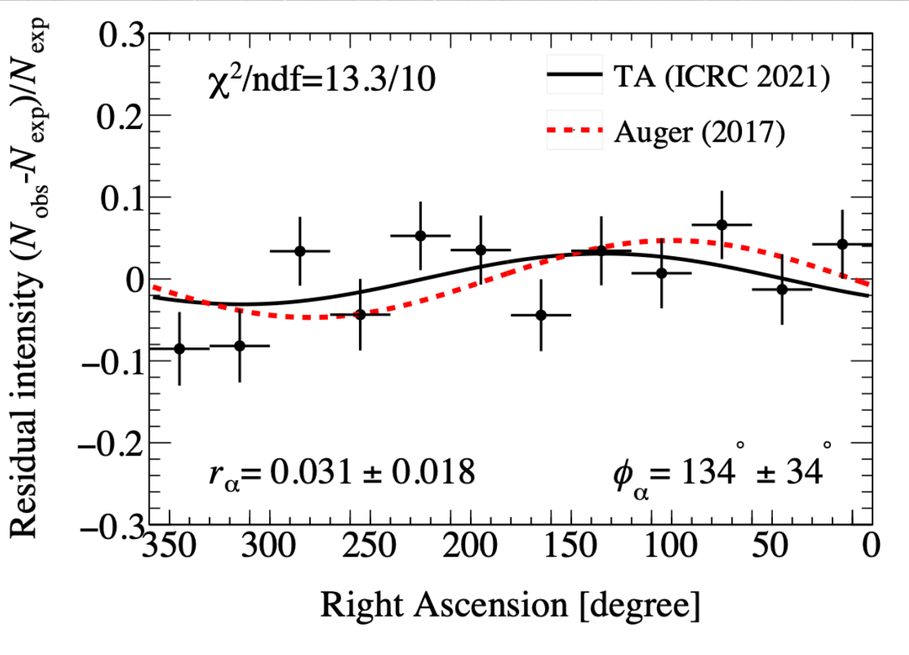

Telescope Array,
Toshihiro Fujii, ICRC'2021

- обнаружение диполя 5σ при E>8 ЭэВ
- согласуется с моделью изотропных источников $\rho = 10^{-4}$ Мпк$^{-3}$

Горячее пятно Telescope Array

Li-Ma Significance Map with E ≥ 57 EeV

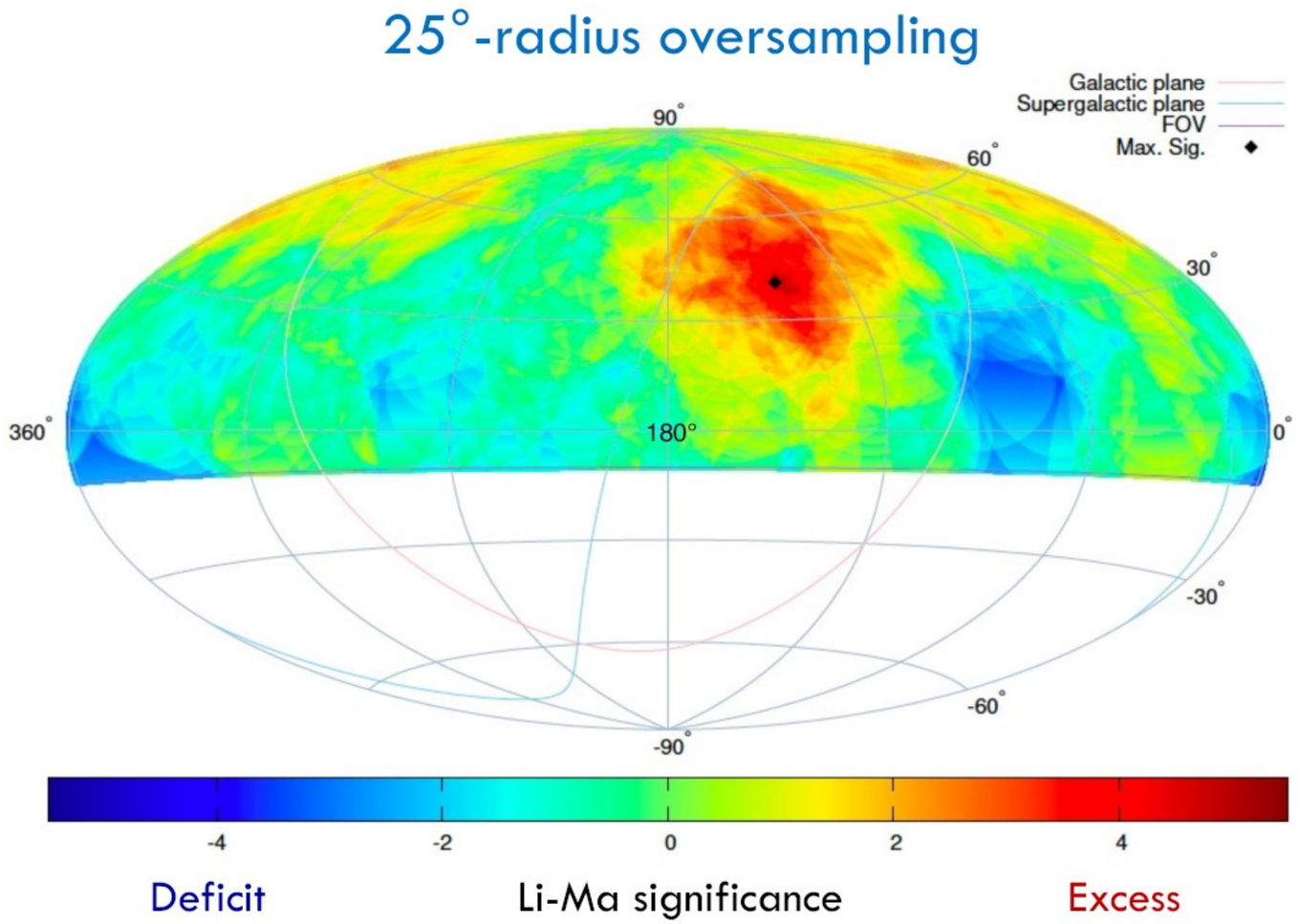

- 205 events (14-year TA SD data)
- Max local sig.: **5.1σ** at (144.0°, 40.5°)

  Obs. : 44 events
  N_{bg} : 16.9 events
  } ~160% excess

- Post-trial probability:

$$P(S_{MC} > 5.1\sigma) = 7.4\times10^{-4} \rightarrow \mathbf{3.2\sigma}$$

Горячее пятно Telescope Array

Independent Dataset Analysis

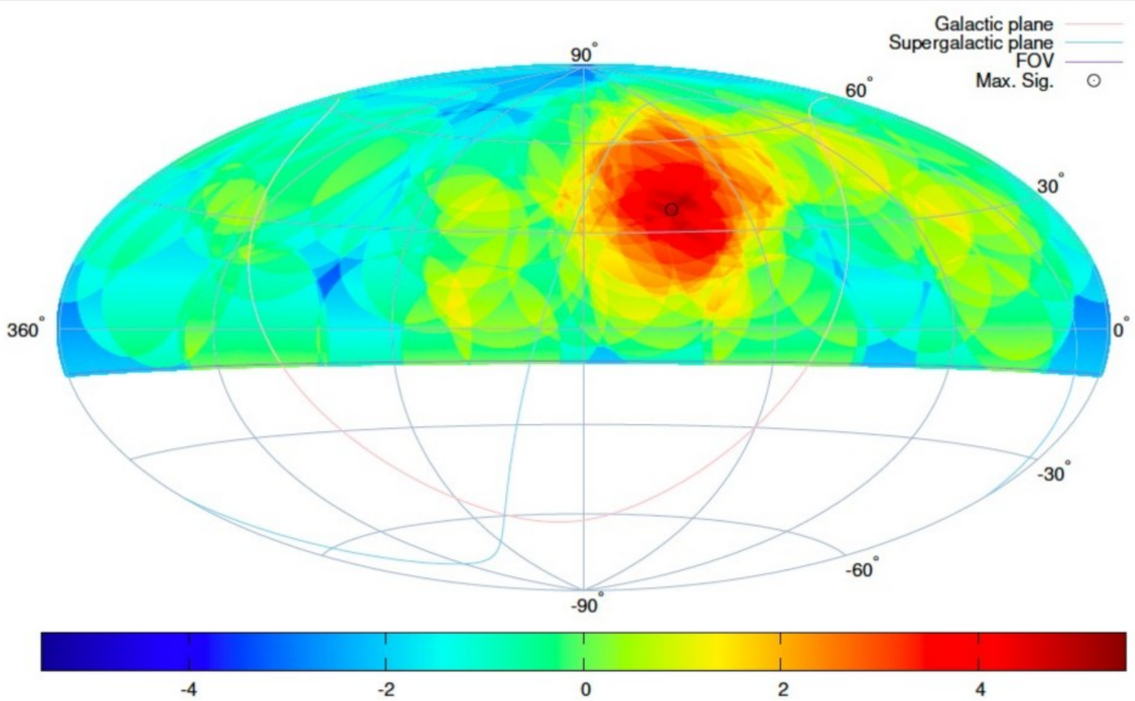

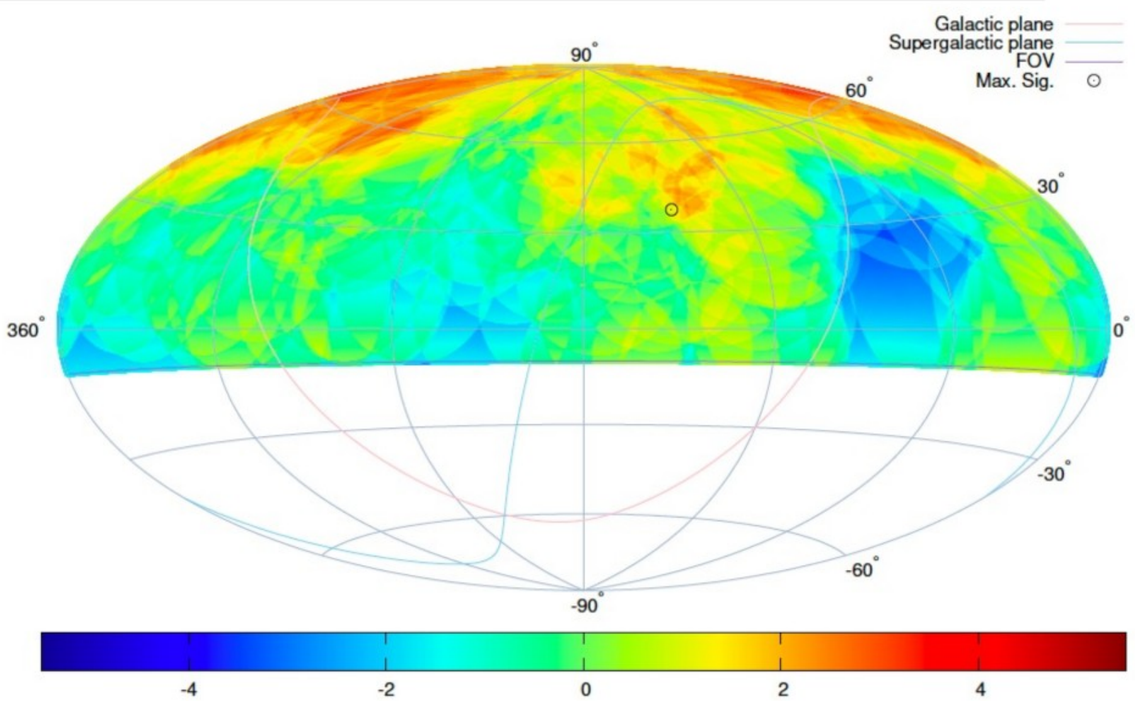

- 72 events (First 5-year)
- **5.0σ** at (144.0°, 40.5°)

  Obs. : 22 events

  N_{bg} : 5.2 events

- 133 events (Last 9-year)
- **2.5σ** at (144.0°, 40.5°)

  Obs. : 22 events

  N_{bg} : 11.6 events

Горячее пятно Telescope Array

Growth of the Hotspot

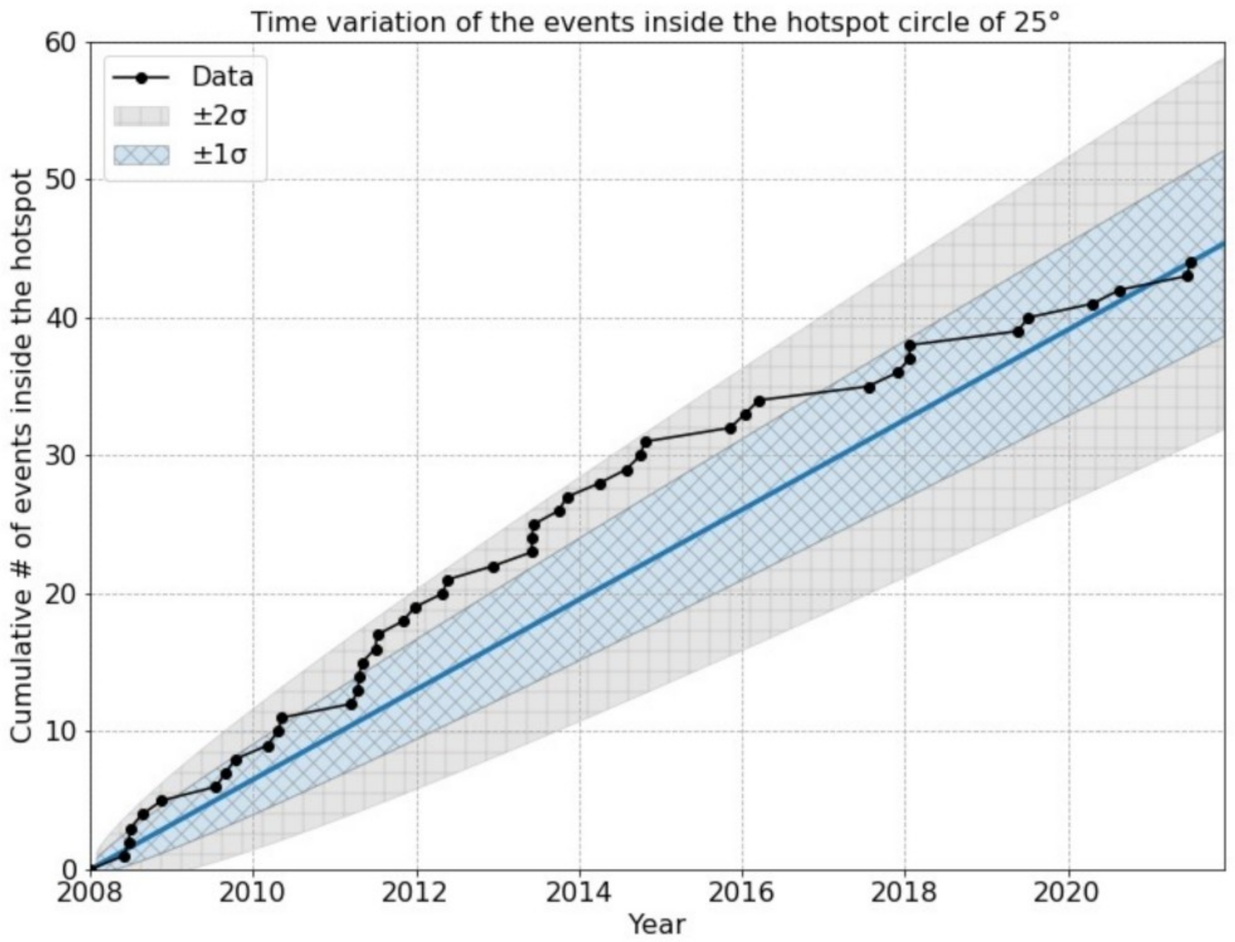

- Black dots: cumulative # of events falling inside the hotspot circle of 25°

- Blue solid line: estimated event rate inside the hotspot

The increase rate of the events inside the hotspot circle is **consistent with the linear increase within ~2σ.**

Горячее пятно Telescope Array

Event Ratio of the Hotspot

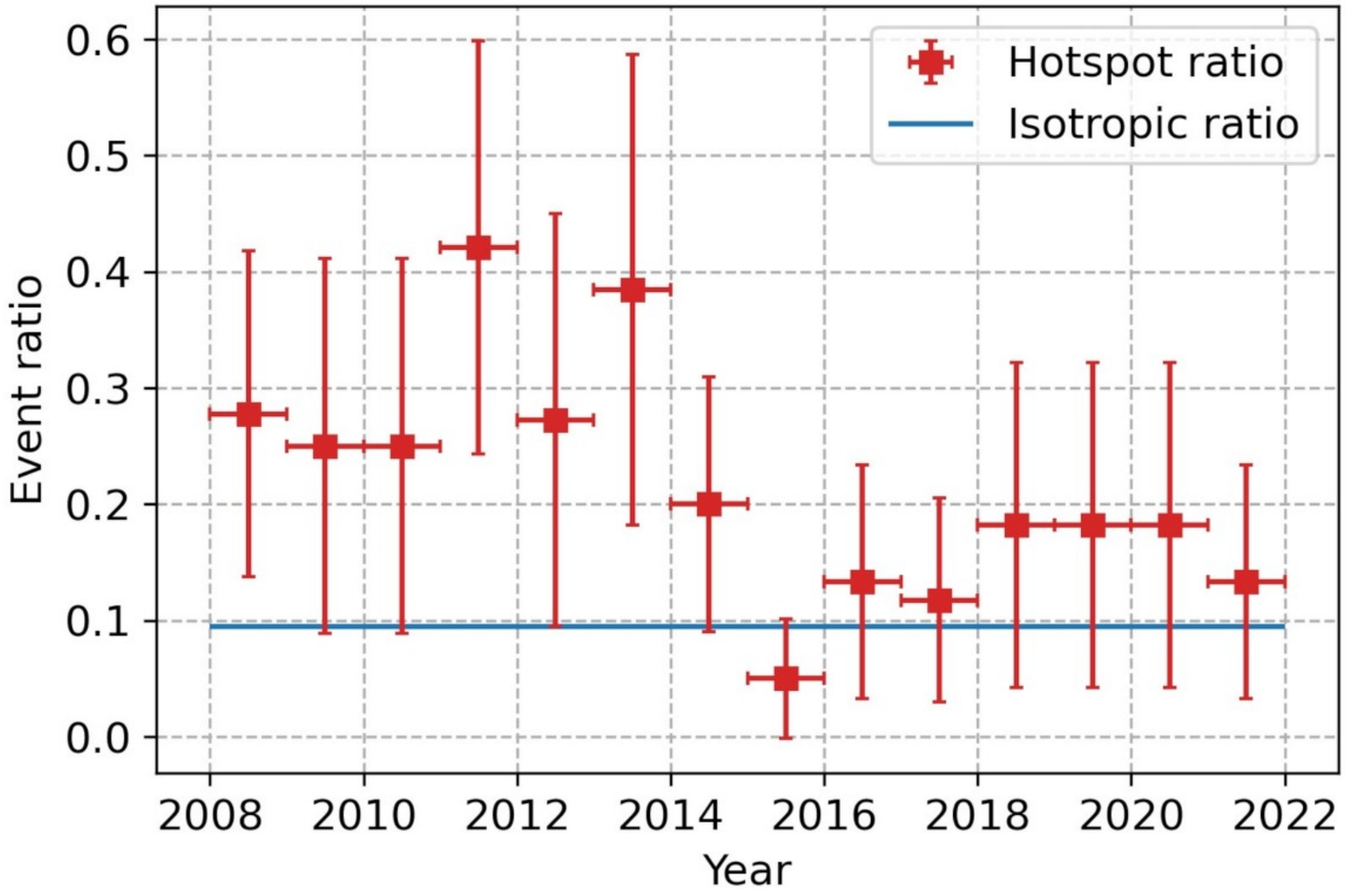

Hotspot ratio:

# of events inside the hotspot/total # of events

Isotropic ratio (Hotspot aperture):

# of isotropic simulation events inside the hotspot / total # of isotropic simulation events (10^5)

(different from the definition of α)

$$\beta = \frac{N_{\mathrm{sim,circle}}}{N_{\mathrm{sim,total}}}$$

$$\alpha = \frac{N_{\mathrm{sim,on}}}{N_{\mathrm{sim,off}}} = \frac{N_{\mathrm{sim,circle}}}{(N_{\mathrm{sim,total}} - N_{\mathrm{sim,circle}})}$$

This plot shows that we observed more events inside the hotspot compared to the isotropic expectation except for one year.

TA: указание на новый избыток

New excess in Slightly Lower Energy Events TA Collab., ICRC2021

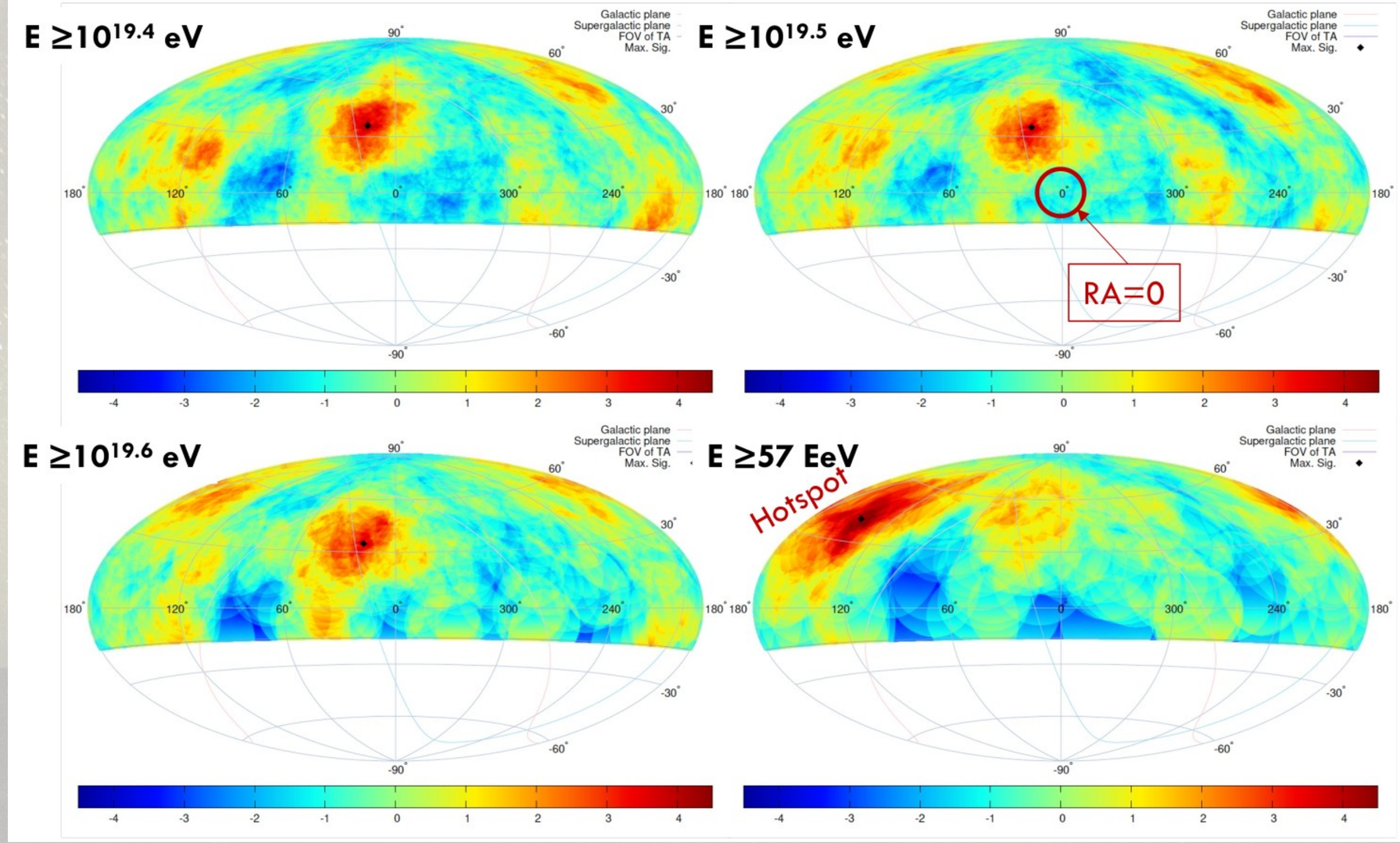

- Li-Ma significance map: excess (red) / deficit (blue) of events compared to isotropy
- Black diamond (◆): the maximum Li-Ma significance position
- Equatorial coords. having RA=0 at center

TA: указание на новый избыток

What is Behind the New Excess?

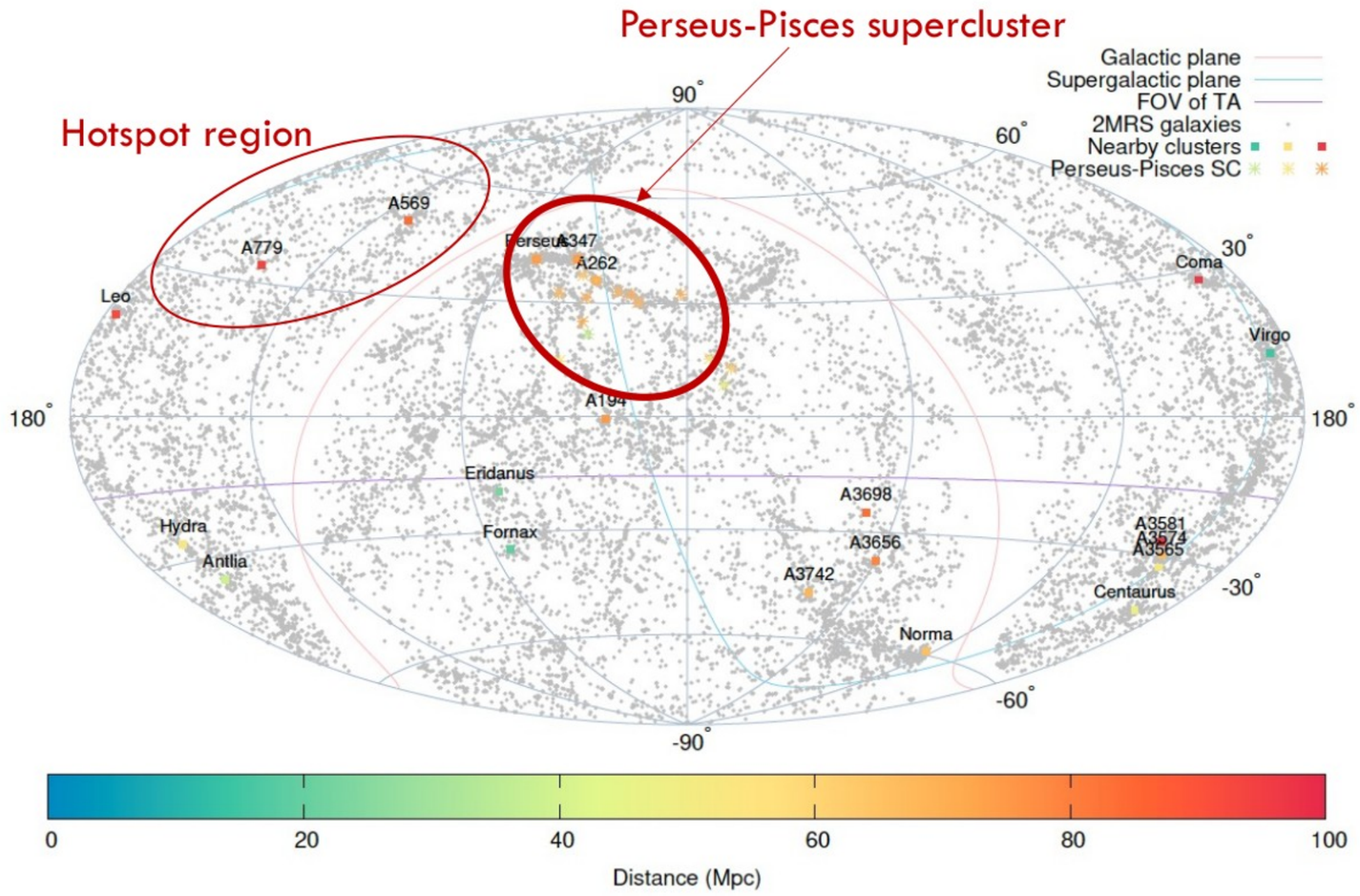

Sky map with nearby galaxies and clusters of galaxies in equatorial coordinates

- Gray dots (·): nearby galaxies from the 2MASS Redshift Survey catalog
- Colored squares (■): nearby clusters of galaxies
- Colored asterisks (*): representative elements of Perseus-Pisces supercluster

Equatorial coordinates

TA: указание на новый избыток

Chance Probability Estimation

- To quantify how often this happens by chance, we generate many Monte-Carlo event sets, each containing the same number of events as the data, thrown isotropically according to the acceptance of the TA SD.
- We count as successes the number of sets where the point of maximum Li-Ma significance is at least as significant as in the data, and also occurs at least as close to the PPSC as in the data: $(S_{mc} \geq S_{obs})$ and $(\theta_{mc} \leq \theta_{obs})$.
- Chance probability of having equal or higher excess on top of the PPSC / major structures {PPSC, Virgo cluster, Coma SC, Leo SC, Hercules SC}

Summary of the Monte-Carlo studies that estimate the chance probability of having an excess

Energy (eV)	Events	Criteria	PPSC	Major structures
$E \geq 10^{19.4}$	1060	$(S_{mc} \geq 3.8\sigma)$ & $(\theta_{mc} \leq 8.6^{\circ})$	3.1σ	2.5σ
$E \geq 10^{19.5}$	685	$(S_{mc} \geq 3.8\sigma)$ & $(\theta_{mc} \leq 7.4^{\circ})$	3.2σ	2.6σ
$E \geq 10^{19.6}$	413	$(S_{mc} \geq 3.5\sigma)$ & $(\theta_{mc} \leq 6.8^{\circ})$	3.0σ	2.4σ

CR clustering: Medium scales

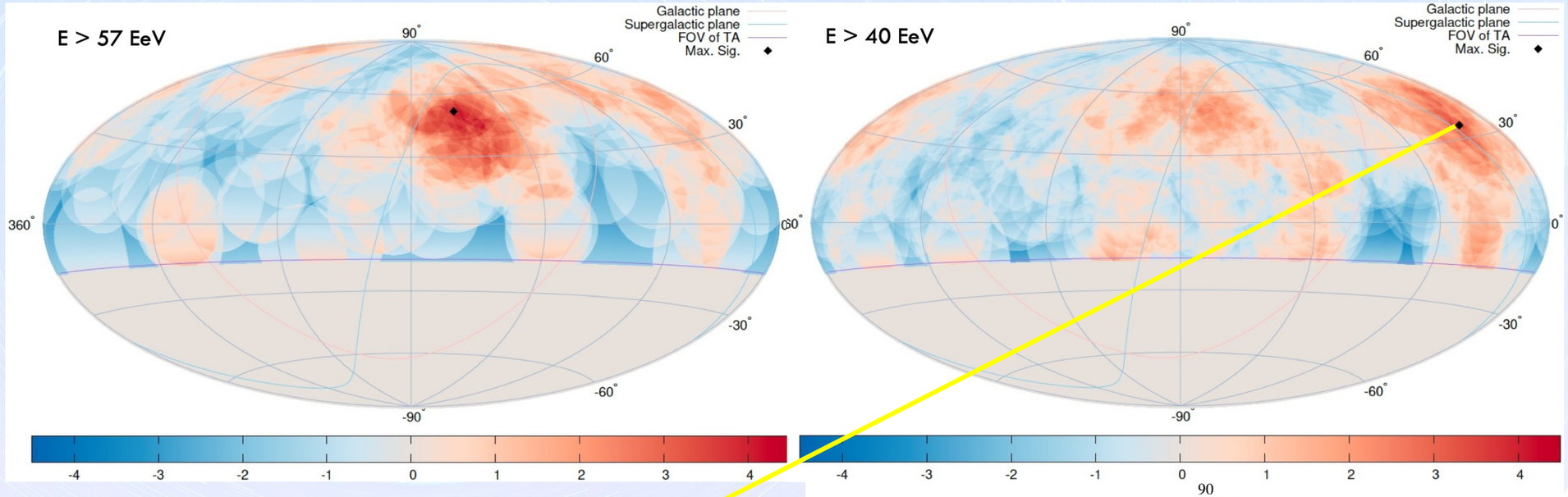

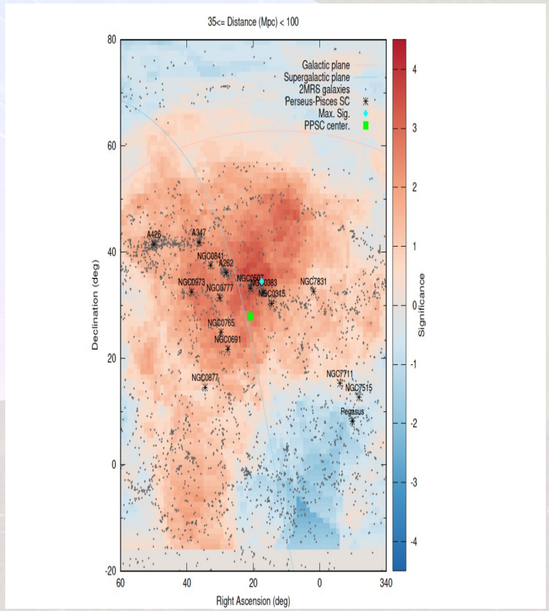

Hint of excess in the direction of Perseus-Pisces supercluster

TA Collaboration, arXiv:2110.14827

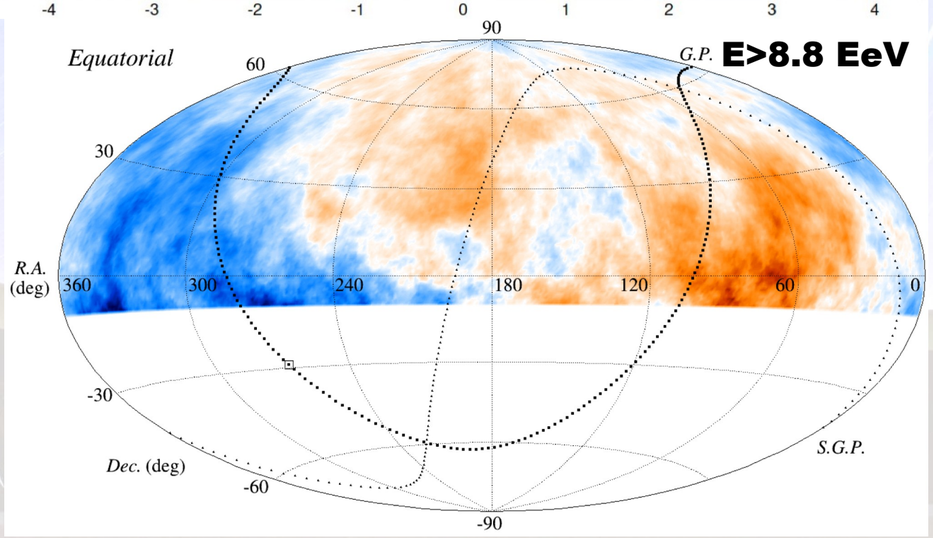

TA: Состав из корреляций с крупномасштабной структурой

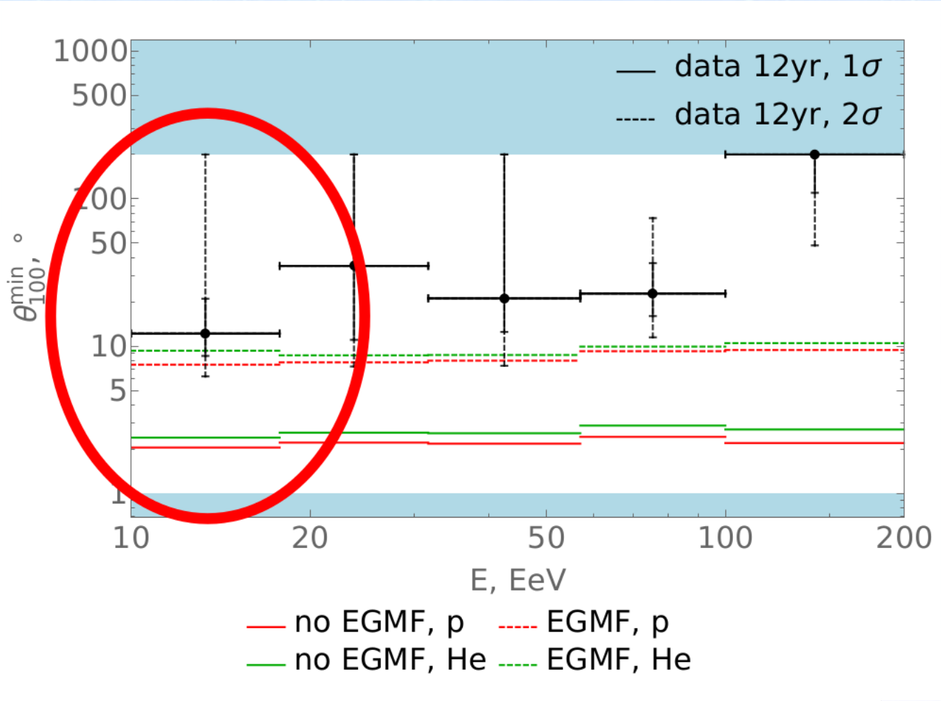

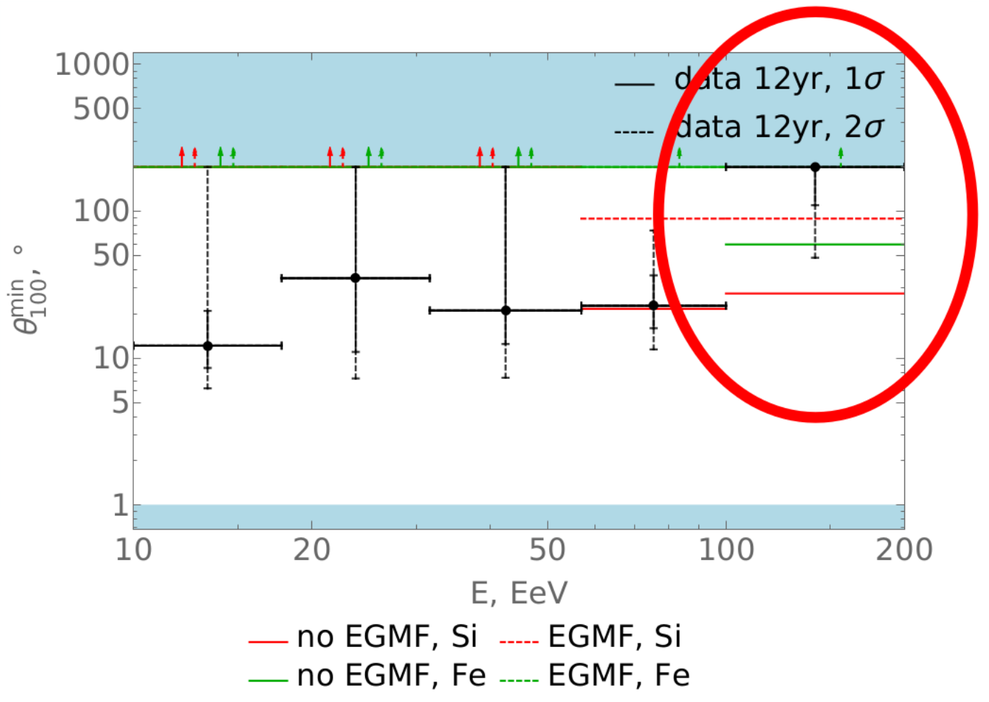

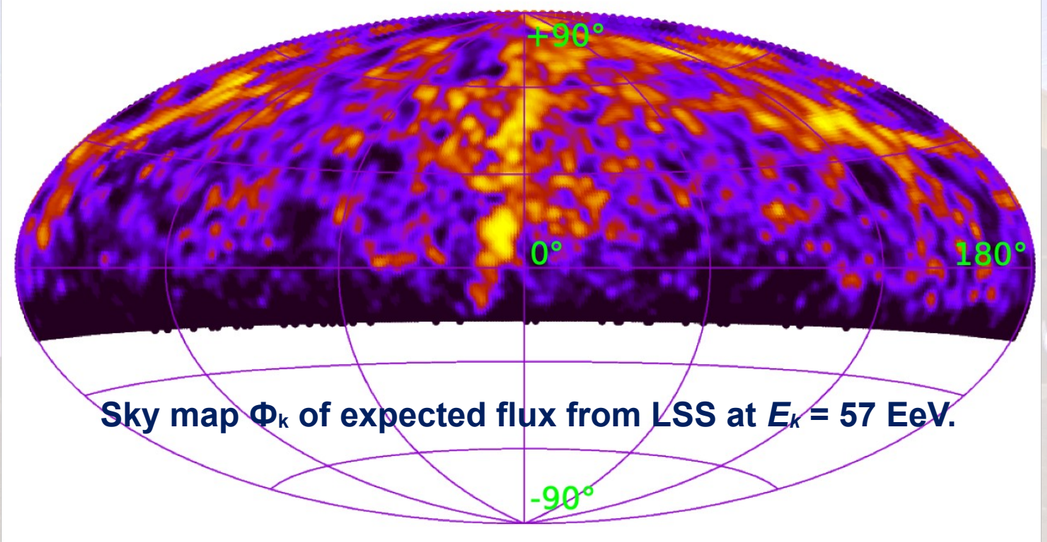

Sky map Φ_k of expected flux from LSS at E_k = 57 EeV.

На самых высоких энергиях — тяжелый состав

Mikhail Kuznetsov, UHECR'2022

TA-Auger: корреляции с галактиками звездообразования

catalogue	$E_{\rm min}^{\rm (Auger)}$	$E_{\rm min}^{\rm (TA)}$	ψ [deg]	f [%]	TS	significance
all galaxies	40 EeV	51 EeV	29^{+11}_{-12}	41^{+29}_{-18}	14.3	$2.7\sigma_{\rm global}$
starburst	38 EeV	49 EeV	$15.1^{+4.6}_{-3.0}$	$12.1^{+4.5}_{-3.1}$	31.1	$4.6\sigma_{\rm global}$

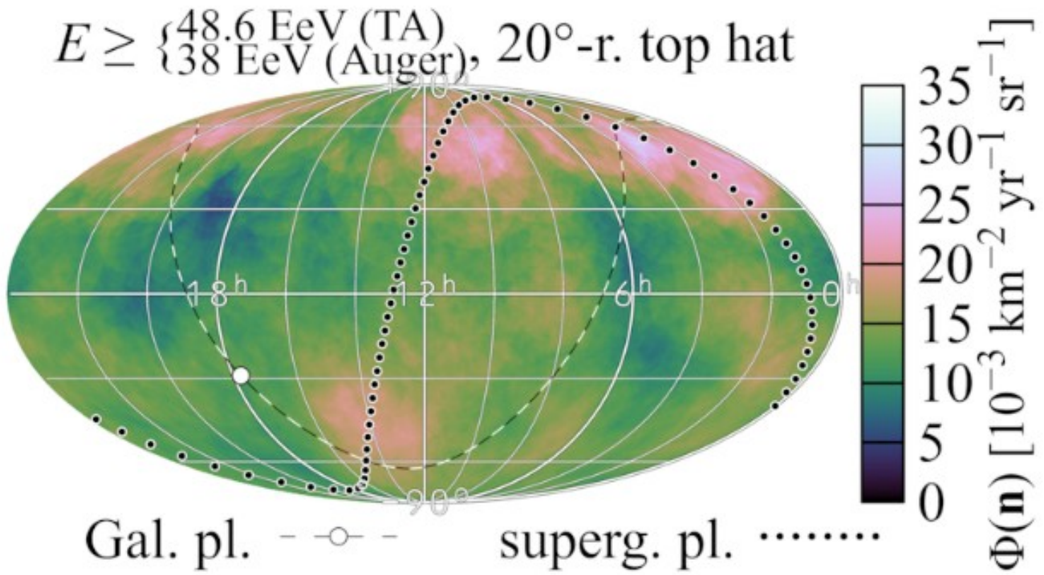

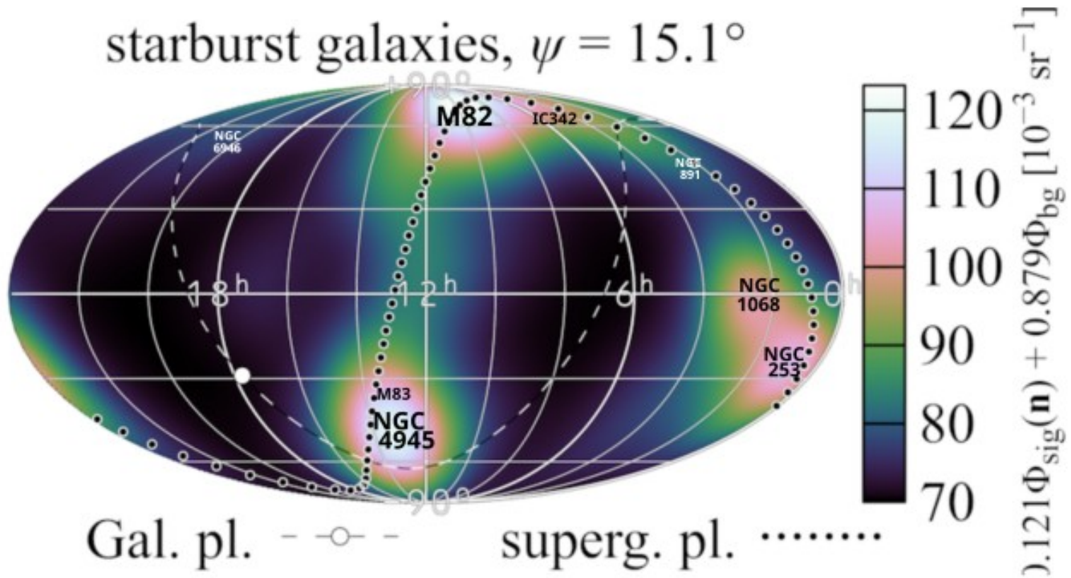

Federico Urban, UHECR'2022

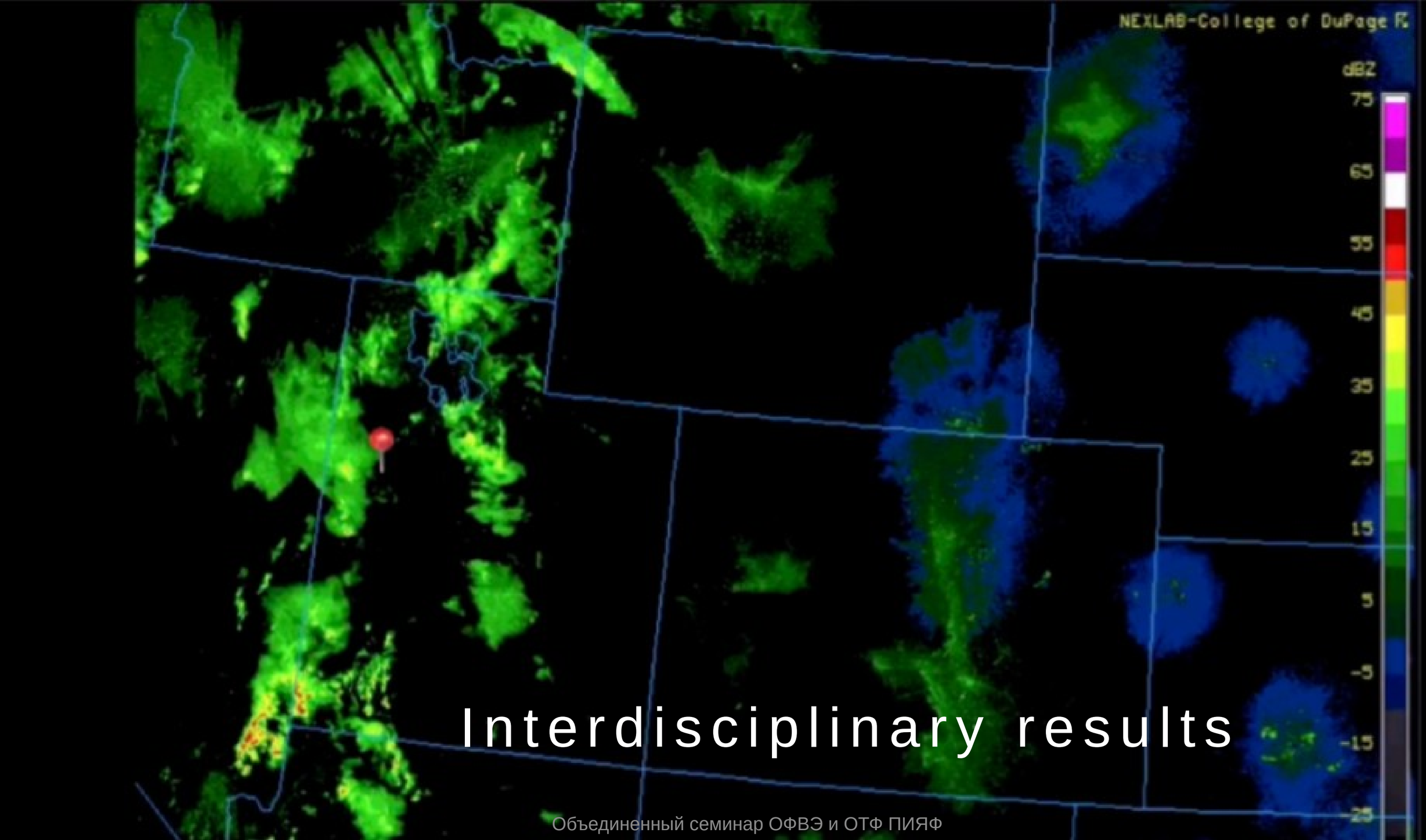

Interdisciplinary results

Observation of Terrestrial Gamma-Ray Flashes with TA SD

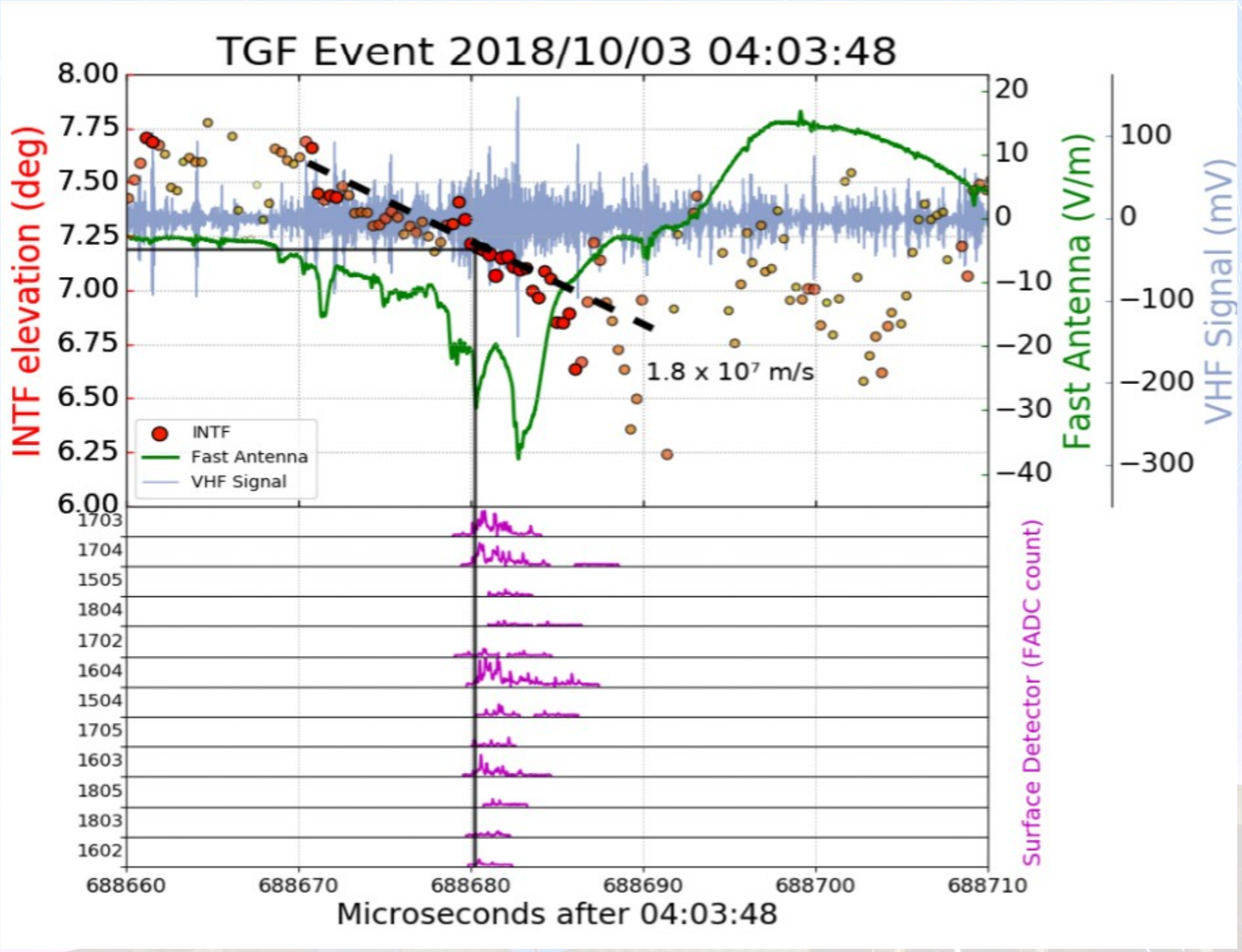

- Broadband Interferometer (INTF):
  - Three 20-80 MHz flatplate antennas
  - 2D high-resolution reconstruction of lightning sources
- Fast Sferic Sensor (FA):
  - Detects electric field change
  - Identifies substructure: initial breakdown pulses (IBPs)

- Clearly defined TGF onset during the flash's strongest initial breakdown pulse

TA Collaboration, arXiv:2205.05115

Variation of Level-0 trigger rate during Thunderstorms

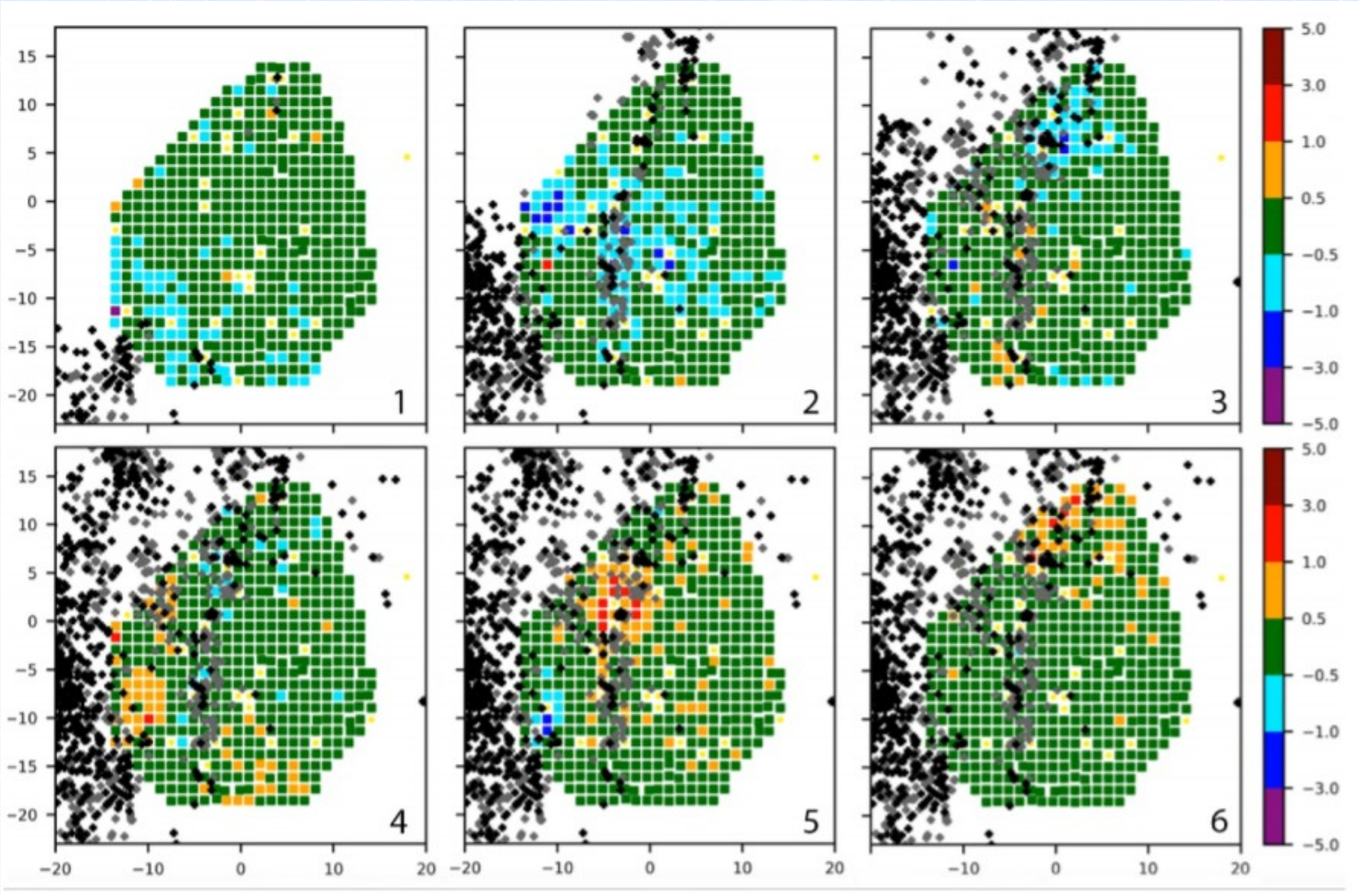

- Level-0 trigger rate is monitored at 10 min resolution at each SD station.
- Thunderstorm detected by NLDN changes the trigger rate.
- The result may be interpreted by using EFIELD option of CORSIKA.
- Intensity increase or deficit depends on electric field type (intracloud or cloud to ground) and thunderstorm polarity

TA Collaboration, Phys. Rev. D 105, 062002

Выводы

- Энергетический спектр измерен в диапазоне от $10^{15.5}$ to $10^{20.5}$ eV (5 декад)
  - Спектр подтверждает эффект Грейзена-Зацепина-Кузьмина
  - Новая особенность в спектре при энергии ~$10^{19.3}$eV
- Положение второго колена в спектре и утяжеление состава между первым и вторым коленом соответствует интерпретации цикла Питерса ($10^{15.6}$eV→$10^{17.1}$eV)
- Измерено сечение протон-азот при энергии в с.ц.м. (pp) 70 ТэВ
- Сильные ограничения на поток фотонов и нейтрино ультравысоких энергий
- Наблюдается избыток мюонов в ШАЛ по сравнению со всеми моделями
- Дипольная анизотропия при E>8x10^{18} эВ (Auger, значимость 5σ)
- Ряд указаний на анизотропию
  - Горячее пятно в направлении на созвездие Большой медведици
  - Указание на избыток в направлении сверхскопления Персея-Рыб, E > $10^{19.3}$eV
  - Наблюдается корреляция направлений прихода с крупномасштабной структурой
- ЭМ каскад, вызванный молнией, может наблюдаться на установках ШАЛ